



Universiteit  
Leiden  
The Netherlands

## TGF- $\beta$ signaling dynamics in epithelial-mesenchymal plasticity of cancer cells

Fan, C.

### Citation

Fan, C. (2024, June 26). *TGF- $\beta$  signaling dynamics in epithelial-mesenchymal plasticity of cancer cells*. Retrieved from <https://hdl.handle.net/1887/3765351>

Version: Publisher's Version

License: [Licence agreement concerning inclusion of doctoral thesis in the Institutional Repository of the University of Leiden](#)

Downloaded from: <https://hdl.handle.net/1887/3765351>

**Note:** To cite this publication please use the final published version (if applicable).



## Chapter 3

### **The lncRNA *LETS1* promotes TGF- $\beta$ -induced EMT and cancer cell migration by transcriptionally activating a T $\beta$ RI-stabilizing mechanism**

Chuannan Fan<sup>1,2</sup>, Román González-Prieto<sup>1,3,4</sup>, Thomas B. Kuipers<sup>5</sup>, Alfred C. O. Vertegaal<sup>1</sup>, Peter A. van Veelen<sup>6</sup>, Hailiang Mei<sup>5</sup>, and Peter ten Dijke<sup>1,2\*</sup>

<sup>1</sup>Department of Cell and Chemical Biology, Leiden University Medical Center, Leiden, The Netherlands.

<sup>2</sup>Oncode Institute, Leiden University Medical Center, Leiden, The Netherlands.

<sup>3</sup>Genome Proteomics laboratory, Andalusian Center for Molecular Biology and Regenerative Medicine (CABIMER), University of Seville, Seville, Spain.

<sup>4</sup>Department of Cell Biology, University of Seville, Seville, Spain

<sup>5</sup>Department of Biomedical Data Sciences, Sequencing Analysis Support Core, Leiden University Medical Center, Leiden, The Netherlands.

<sup>6</sup>Center for Proteomics and Metabolomics, Leiden University Medical Center, Leiden, The Netherlands.

\*Corresponding author. Tel: +31 71 526 9271; Fax: +31 71 526 8270; E-mail: p.ten\_dijke@lumc.nl

## Abstract

Transforming growth factor- $\beta$  (TGF- $\beta$ ) signaling is a critical driver of epithelial-to-mesenchymal transition (EMT) and cancer progression. In SMAD-dependent TGF- $\beta$  signaling, activation of the TGF- $\beta$  receptor complex stimulates the phosphorylation of the intracellular receptor-associated SMADs (SMAD2 and SMAD3), which translocate to the nucleus to promote target gene expression. SMAD7 inhibits signaling through the pathway by promoting the polyubiquitination of the TGF- $\beta$  type I receptor (T $\beta$ RI). We identified an unannotated nuclear long noncoding RNA (lncRNA) that we designated *LETS1* (lncRNA enforcing TGF- $\beta$  signaling 1) that was not only increased but also perpetuated by TGF- $\beta$  signaling. Loss of *LETS1* attenuated TGF- $\beta$ -induced EMT and migration in breast and lung cancer cells *in vitro* and extravasation of the cells in a zebrafish xenograft model. *LETS1* potentiated TGF- $\beta$ -SMAD signaling by stabilizing cell surface T $\beta$ RI, thereby forming a positive feedback loop. Specifically, *LETS1* inhibited T $\beta$ RI polyubiquitination by binding to nuclear factor of activated T cells (NFAT5) and inducing the expression of the gene encoding the orphan nuclear receptor 4A1 (NR4A1), a component of a destruction complex for SMAD7. Overall, our findings characterize *LETS1* as an EMT-promoting lncRNA that potentiates signaling through TGF- $\beta$  receptor complexes.

## Introduction

Epithelial-to-mesenchymal transition (EMT) is a cellular transdifferentiation process in which epithelial cells lose their cell-cell adhesions and gain the traits of mesenchymal cells<sup>1</sup>. This process is characterized by the loss of the epithelial marker E-cadherin and the induction of mesenchymal markers such as N-cadherin and Vimentin. Cancer cells undergoing EMT acquire migratory and invasive properties and become resistant to chemotherapy<sup>2,3</sup>. Several intermediate states, termed as partial or hybrid EMT states, occur during EMT of cancer cells<sup>4</sup>. Because the process is highly dynamic and reversible, these cancer cells demonstrate a high amount of plasticity and exhibit increased aggressiveness<sup>4-7</sup>. Moreover, the hybrid EMT RNA signature is correlated with a poor patient prognosis in multiple cancer types<sup>8-10</sup>.

Transforming growth factor- $\beta$  (TGF- $\beta$ ) signaling plays a crucial role in cancer cell progression through the induction of EMT<sup>11,12</sup>. Binding of TGF- $\beta$  ligands enables the TGF- $\beta$  type II serine-threonine kinase receptor (T $\beta$ RII) to activate the type I receptor (T $\beta$ RI), which induces phosphorylation of SMAD2 and SMAD3 (SMAD2/3). Upon forming complexes with SMAD4, activated SMAD2/3 translocate into the nucleus to regulate target gene transcription<sup>13,14</sup>. TGF- $\beta$  signaling is tightly controlled at multiple levels<sup>15,16</sup>. The E3 ligase SMAD ubiquitination regulatory factor 2 (SMURF2) is recruited by inhibitory SMAD7 to target T $\beta$ RI for polyubiquitination and degradation<sup>17</sup>. SMAD7 itself is also fine-tuned by polyubiquitination directed by various E3 ligases, including ARKADIA and ring finger protein 12 (RNF12)<sup>18,19</sup>. Moreover, the orphan nuclear receptor 4A1 (NR4A1) interacts with complexes composed of AXIN2 and RNF12 or ARKADIA to facilitate SMAD7 polyubiquitination and subsequent proteasomal and lysosomal degradation<sup>20</sup>.

Long noncoding RNAs (lncRNAs) are emerging as critical players in modulating signaling transduction and cancer progression<sup>21-23</sup>. As a family of noncoding RNAs that are longer than 200 nucleotides in length, lncRNAs can act as scaffolds, guides, or decoys to alter protein-protein interactions or the accessibility of proteins to DNA, thereby enabling them to change signaling transduction at multiple levels<sup>24,25</sup>. MicroRNAs can be sponged by lncRNAs through the competitive endogenous RNA mechanism<sup>26,27</sup>. TGF- $\beta$ -induced responses can be regulated by the induction of certain lncRNAs that serve as effectors<sup>28,29</sup>. Moreover, the expression or activity of TGF- $\beta$  signaling components is altered by lncRNAs acting as modulators<sup>30-34</sup>. To

identify additional lncRNAs that participate in TGF- $\beta$ -induced EMT and cancer progression, we performed a transcriptome screen in three breast cell lines and identified 15 lncRNAs whose expression can be induced by TGF- $\beta$ -SMAD signaling. One of these TGF- $\beta$ -induced lncRNAs, *LITATS1*, inhibits TGF- $\beta$  signaling and TGF- $\beta$ -induced EMT by promoting the degradation of T $\beta$ RI<sup>35</sup>. Here, we focused on an unannotated lncRNA that we named *LETS1* (lncRNA enforcing TGF- $\beta$  signaling 1), because it promoted TGF- $\beta$ -SMAD signaling and TGF- $\beta$ -induced EMT, migration, and extravasation in breast and lung cancer cells. *LETS1* knockdown enhanced polyubiquitination of T $\beta$ RI. Mechanistically, *LETS1* induced *NR4A1* expression by interacting with nuclear factor of activated T cells (NFAT5) and potentiating NFAT5-mediated *NR4A1* transcription. These findings reveal another layer of T $\beta$ RI signaling regulation by a previously uncharacterized lncRNA. Targeting *LETS1* may provide a promising therapeutic opportunity to restrain overly active TGF- $\beta$  signaling in EMT and cancer progression.

## Results

### ***LETS1* is a nuclear lncRNA induced by TGF- $\beta$ -SMAD signaling**

We previously reported on lncRNAs that are potently induced by TGF- $\beta$  by performing transcriptional profiling of three breast cell lines: nonmalignant MCF10A-M1 cells, premalignant MCF10A-M2 cells, and MDA-MB-231 adenocarcinoma cells (fig. S1A)<sup>35</sup>. In this study, we focused on the TGF- $\beta$ -induced lncRNA *LETS1* for further investigation (fig. S1A). To characterize *LETS1*, we first confirmed the induction of *LETS1* by TGF- $\beta$  in A549 lung adenocarcinoma cells and breast cell lines (Fig. 1A). To test whether TGF- $\beta$ -induced *LETS1* expression was mediated by the canonical SMAD pathway, we knocked down *SMAD2*, *SMAD3*, or *SMAD4* using independent short hairpin RNA(s) [shRNA(s)] in MDA-MB-231 cells (fig. S1B). We observed that TGF- $\beta$ -induced *LETS1* expression was greatly attenuated upon depletion of *SMAD2*, *SMAD3*, or *SMAD4* (Fig. 1B). Moreover, TGF- $\beta$  increased *LETS1* expression in MDA-MB-231 cells that were pretreated with cycloheximide (CHX), implying that new protein synthesis was not required for TGF- $\beta$  to induce *LETS1* expression (fig. S1C). We then mapped the *LETS1* locus on chromosome 15 [chromosome 15: 82098836 to 82101500 (GRCh38.p14)] and revealed that *LETS1* was a single-exon intergenic transcript using 5' and 3' rapid amplification of cDNA ends (RACE) assays (Fig. 1C and fig. S1D). Sequence similarity search by the Basic Local Alignment Search Tool<sup>36</sup> showed that the sequence of *LETS1* is unique in the human transcriptome. We evaluated the coding potential of *LETS1* using the Coding Potential Assessment Tool (CPAT)<sup>37</sup>, which predicted a lack of coding capability for *LETS1* as compared with other protein-coding mRNAs [*ACTB2* and *GAPDH* (glyceraldehyde-3-phosphate dehydrogenase); fig. S1E]. Reverse transcription quantitative polymerase chain reaction (RT-qPCR) after subcellular fractionation in the three breast cell lines revealed that *LETS1* was predominantly localized in the nucleus (Fig. 1D). In addition, fluorescence in situ hybridization using a specific *LETS1* probe showed that TGF- $\beta$  stimulation enhanced the *LETS1* nuclear signal, which was strongly decreased upon GapmeR-mediated *LETS1* depletion in MDA-MB-231 cells (Fig. 1E). Together, these results demonstrated that *LETS1* is a TGF- $\beta$ -SMAD-induced lncRNA mainly localized in the nucleus.

### ***LETS1* promotes TGF- $\beta$ -induced EMT, migration, and extravasation of cancer cells**

Because the products of TGF- $\beta$ -SMAD signaling target genes frequently function as modulators or effectors of TGF- $\beta$ -SMAD signaling, we determined whether *LETS1* influenced TGF- $\beta$ -induced EMT in cancer cells. Depletion of *LETS1* transcripts by CRISPR-CasRx attenuated the TGF- $\beta$ -induced decrease in E-cadherin and increase in N-cadherin, Vimentin, and the EMT-promoting transcription factor SNAIL in A549 cells (Fig. 2A and fig. S2, A and B).

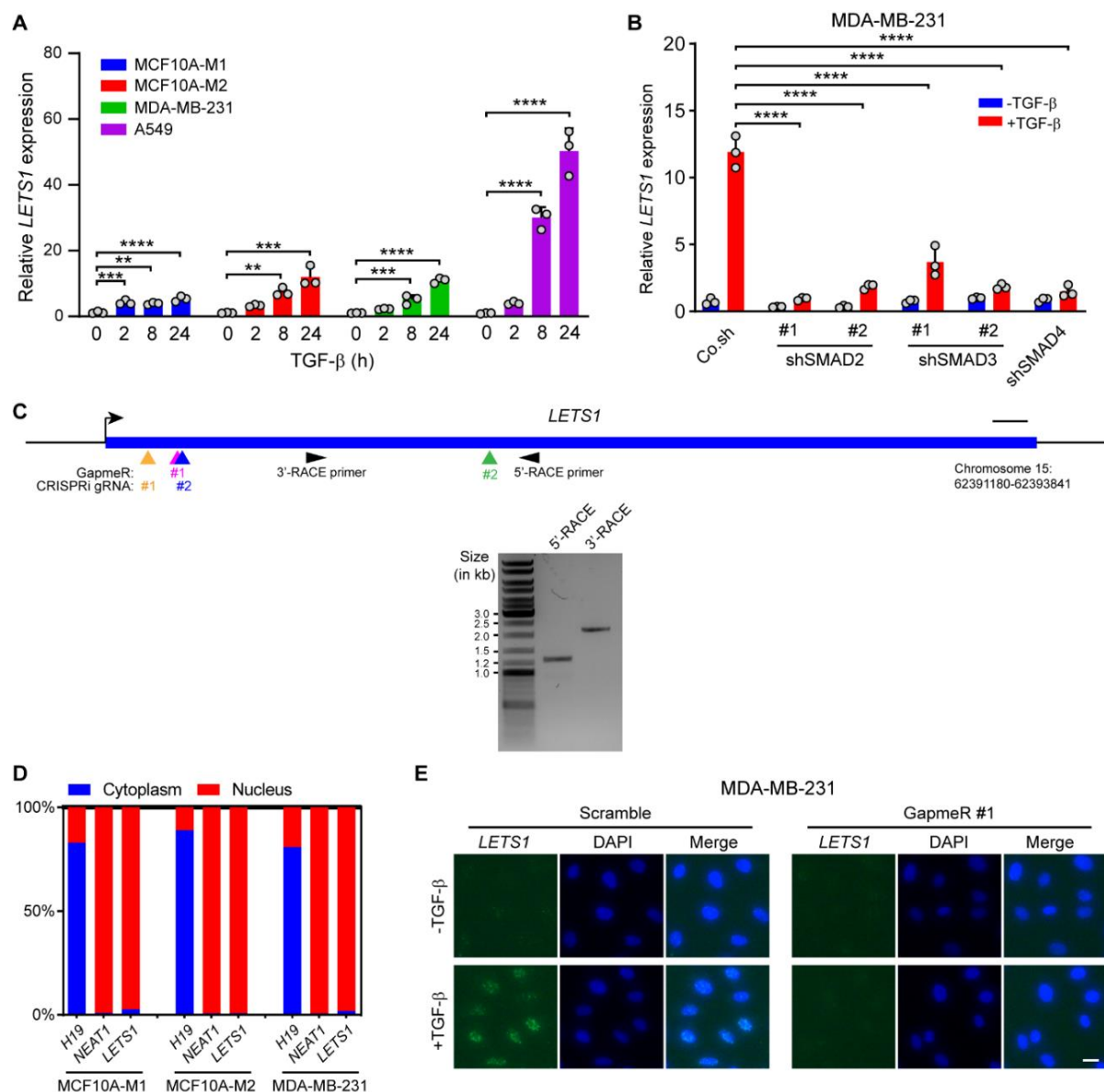


**Fig. 1. *LETS1* is a nuclear lncRNA induced by TGF- $\beta$ -SMAD signaling.** (A) *LETS1* expression was measured by RT-qPCR in MCF10A-M1, MCF10A-M2, MDA-MB-231, and A549 cells. Cells were either not stimulated (0 hour) or stimulated with TGF- $\beta$  for 2, 8, and 24 hours. (B) *LETS1* expression was measured by RT-qPCR in MDA-MB-231 cells upon shRNA-mediated *SMAD2*, *SMAD3*, or *SMAD4* knockdown. Co.sh, empty vector for shRNA expression. RT-qPCR results in (A) and (B) are shown as means  $\pm$  SD from three biological replicates in one independent experiment and representative of at least three independent experiments. (C) Schematic illustration of the *LETS1* locus and the targeting regions of RACE primers, *LETS1*-targeting GapmeRs, and *LETS1*-targeting CRISPRi guide RNAs (gRNAs). Scale bar, 100 bps. *LETS1* 5' - and 3' -RACE DNA products were analyzed by agarose gel electrophoresis. (D) Subcellular distribution of lncRNAs *HI9*, *NEAT1*, and *LETS1* based on RT-qPCR of the cytoplasmic and nuclear fractions of MCF10A-M1, MCF10A-M2, and MDA-MB-231 cells. Results are shown as means and representative of at least three independent experiments. The total amount of each lncRNA was set to 100%. (E) *LETS1* expression and subcellular localization was evaluated by RNA fluorescence in situ hybridization in MDA-MB-231 cells. Nuclei were stained with DAPI. Scale bar, 40  $\mu$ m. In (A) and (B), significance was assessed using one-way analysis of variance (ANOVA) followed by Dunnett's multiple comparisons test. \*\*, 0.001 <  $P$  < 0.01; \*\*\*, 0.0001 <  $P$  < 0.001; \*\*\*\* $P$  < 0.0001.

In addition, *LETS1* knockdown alleviated TGF- $\beta$ -induced filamentous (F)-actin formation in A549 cells (fig. S2C). The suppressive effect of *LETS1* knockdown on EMT was further confirmed by blocking *LETS1* transcription in MCF10A-M2 cells using CRISPR interference (CRISPRi) (fig. S2, D and E). In contrast, ectopic *LETS1* expression potentiated TGF- $\beta$ -induced EMT marker expression in A549 cells (Fig. 2B and fig. S2, F and G). Transcriptional

profiling and gene set enrichment analysis (GSEA) also validated the positive correlation between the manipulation of *LETS1* expression and the EMT gene signature (Fig. 2C).

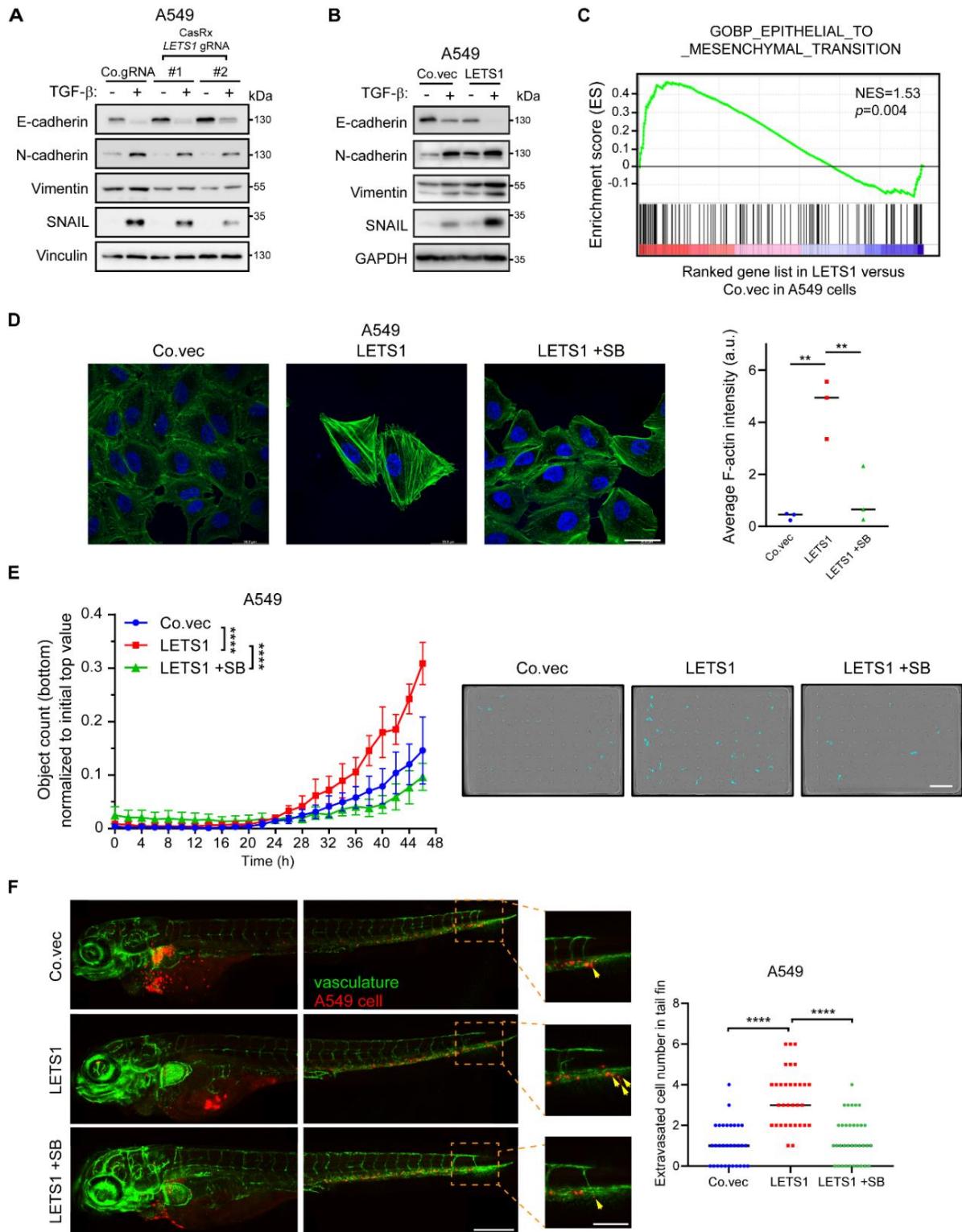


**Fig. 2. *LETS1* promotes TGF- $\beta$ -induced EMT, migration, and extravasation in cancer cells.** (A and B) Immunoblotting for E-cadherin, N-cadherin, vimentin, and SNAIL in A549 cells expressing CRISPR-CasRx construct and empty vector (Co.gRNA) or *LETS1*-targeting gRNA (A) and in A549 cells overexpressing *LETS1* or empty vector (Co.vec) (B). Vinculin and GAPDH are loading controls. Blots are representative of at least three independent experiments. (C) GSEA of the correlation between experimentally manipulated *LETS1* expression and the EMT gene signature in A549 cells. NES, normalized enrichment score. (D) Fluorescent staining for F-actin in A549 cells overexpressing *LETS1* or empty vector

(Co.vec). DAPI staining was performed to visualize nuclei. Scale bar, 38.8  $\mu\text{m}$ . Quantification of average F-actin intensity is shown as means  $\pm$  SD from three independent experiments. a.u., arbitrary units. (E) An IncuCyte chemotactic migration assay was performed with A549 cells overexpressing *LETS1* and treated with SB431542 (SB) or vehicle during the migration assays. Cells that migrated to the bottom chambers are marked in blue in the images. The migration results are expressed as means  $\pm$  SD from four biological replicates in one independent experiment and representative of at least three independent experiments. Scale bar, 400  $\mu\text{m}$ . (F) *In vivo* zebrafish extravasation experiments with A549 cells stably expressing mCherry (red) and the *LETS1* expression construct or empty vector (Co.vec). A549 cells were injected into zebrafish embryos expressing enhanced green fluorescent protein (EGFP) throughout the vasculature and treated with vehicle or SB431542 (SB). Extravasated lung cancer cells in the zoomed tail fin area are indicated with yellow arrows. Numbers of extravasated cells are expressed as means  $\pm$  SD. Scale bars, 309.1 (whole fish) and 154.5  $\mu\text{m}$  (enlargements). N = at least 30 fish per treatment group. In (C), significance was assessed by Kolmogorov-Smirnov test. In (D) and (F), significance was assessed using one-way ANOVA followed by Dunnett's multiple comparisons test. In (E), significance was assessed using two-way ANOVA followed by Tukey's multiple comparisons test. \*\*, 0.001 < P < 0.01; \*\*\*\*P < 0.0001.

To test the effect of *LETS1* on cell migration, we performed chemotactic migration assays in MDA-MB-231 cells. As expected, CRISPRi-mediated *LETS1* knockdown alleviated TGF- $\beta$ -induced cell migration (fig. S3A). In agreement with this result, *LETS1* depletion resulted in a decrease of MDA-MB-231 cell extravasation in a zebrafish xenograft cancer model (fig. S3B). On the contrary, *LETS1* ectopic expression promoted F-actin formation, migration, and extravasation in A549 cells (Fig. 2, D to F). Of note, TGF- $\beta$  signaling blockage using the selective T $\beta$ RI kinase inhibitor SB431542 (SB) mitigated the tumor-promoting effect of *LETS1* overexpression on A549 cells (Fig. 2, D to F). These findings indicate that *LETS1* is a pivotal potentiator of TGF- $\beta$ -induced EMT, migration, and extravasation in lung and breast cancer cells.

### ***LETS1* potentiates TGF- $\beta$ -SMAD signaling**

Because the results above suggested that *LETS1* may act as a modulator of TGF- $\beta$  signaling, we investigated the effect of *LETS1* on TGF- $\beta$ -SMAD signaling transduction. We observed that CRISPRi-mediated *LETS1* knockdown reduced, whereas *LETS1* ectopic expression enhanced, the activity of a highly selective synthetic reporter of transcription driven by SMAD3 and SMAD4 (SMAD3/4)<sup>38</sup> in HepG2 cells (Fig. 3A). Consistently, ectopic *LETS1* expression potentiated transcriptional activity of a SMAD3/4-driven dynamic green fluorescent protein (GFP) reporter (Fig. 3B)<sup>39</sup>. Moreover, GapmeR-mediated *LETS1* knockdown suppressed the expression of TGF- $\beta$ -induced target genes (*PAI-1*, *CTGF*, and *SMAD7*) in MDA-MB-231 and A549 cells (Fig. 3C and fig. S4A). However, ectopic *LETS1* expression promoted the TGF- $\beta$ -SMAD-induced transcriptional events, as shown by the increase in TGF- $\beta$  target gene expression and the positive correlation between manipulated *LETS1* expression and the TGF- $\beta$  gene response signature<sup>40</sup> in A549 cells (Fig. 3, D and E). Furthermore, *LETS1* knockdown decreased, whereas *LETS1* overexpression increased, the TGF- $\beta$ -induced SMAD2 phosphorylation in MDA-MB-231, A549, and MCF10A-M2 cells (Fig. 3, F and G; and fig. S4, B and C).

### ***LETS1* inhibits T $\beta$ RI polyubiquitination and promotes T $\beta$ RI stability by inducing *NR4A1* expression**

Given that *LETS1* potentiated TGF- $\beta$  signaling upstream of SMAD2 phosphorylation, we tested the effect of *LETS1* on T $\beta$ RI, the TGF- $\beta$  receptor that directly mediates SMAD2/3 activation. Although the total T $\beta$ RI protein abundance remained unaffected, the amount of T $\beta$ RI at the plasma membrane was significantly reduced in the absence of *LETS1* in MDA-MB-231 cells (Fig. 4A and fig. S5A). Consistent with this notion, we found that T $\beta$ RI polyubiquitination was increased upon *LETS1* knockdown, whereas *LETS1* overexpression reduced T $\beta$ RI polyubiquitination in MDA-MB-231 cells (Fig. 4B and fig. S5B). Considering the nuclear localization of *LETS1*, we hypothesized that the transcription of TGF- $\beta$ -SMAD signaling modulators may be altered by *LETS1*. To screen for relevant *LETS1* target genes, we

The lncRNA *LETS1* promotes TGF- $\beta$ -induced EMT and cancer cell migration by transcriptionally activating a T $\beta$ RI-stabilizing mechanism

analyzed the changes in the transcriptional profile of A549 cells upon ectopic *LETS1* expression. As expected, transcripts of multiple TGF- $\beta$  target genes, including *FOSB*, *COL1A1*, *JUN*, *JUNB*, *ATF3*, and *SNAIL*, were significantly increased by ectopic *LETS1* expression (Fig. 4C).

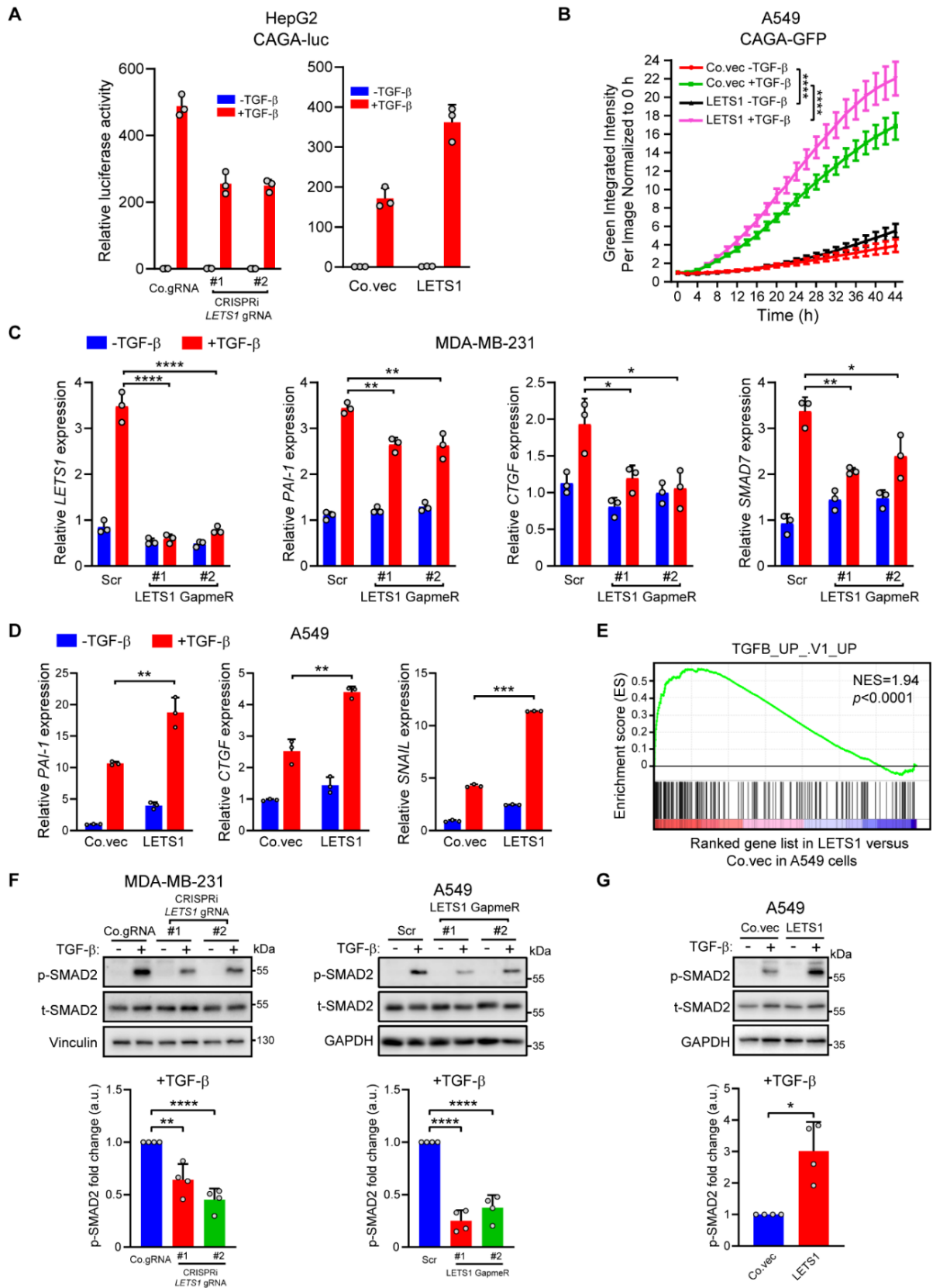




**Fig. 3. *LETSI* potentiates TGF- $\beta$ /SMAD signaling.** (A) Quantification of luciferase activity in HepG2 cells expressing the synthetic SMAD3/4-responsive reporter CAGA-luc and either the *LETSI*-targeting CRISPRi gRNA construct or the *LETSI* overexpression construct and stimulated with TGF- $\beta$  or vehicle. Co.gRNA and Co.vec are the corresponding empty vectors. The relative luciferase activities are representative of at least three independent experiments and expressed as means  $\pm$  SD from three wells of cells per treatment group in one experiment. (B) Quantification of GFP fluorescence in A549 cells coexpressing the CAGA-GFP reporter and either empty vector (Co.vec) or *LETSI* overexpression construct and stimulated with TGF- $\beta$  or vehicle. The results are expressed as means  $\pm$  SD from six biological replicates in one independent experiment and representative of two independent experiments. (C) Quantification of *LETSI*, *PAI-1*, *CTGF*, and *SMAD7* expression in MDA-MB-231 cells transfected with GapmeRs targeting *LETSI* and treated with TGF- $\beta$  or vehicle. Scr, scrambled GapmeR. RT-qPCR results are shown as means  $\pm$  SD from three biological replicates in one independent experiment and representative of at least three independent experiments. (D) Quantification of *PAI-1*, *CTGF*, and *SNAIL* expression in A549 cells overexpressing *LETSI* or empty vector and treated with TGF- $\beta$  or vehicle. RT-qPCR results are shown as means  $\pm$  SD from three biological replicates in one independent experiment and representative of at least three independent experiments. (E) GSEA of correlation between experimentally manipulated *LETSI* expression and the TGF- $\beta$  gene response signature in A549 cells. NES, normalized enrichment score. Significance was assessed by Kolmogorov-Smirnov test. (F and G) Immunoblotting for phosphorylated (p-) and total (t-)SMAD2 in TGF- $\beta$ -stimulated MDA-MB-231 or A549 cells in which *LETSI* was knocked down by CRISPRi (MDA-MB-231) or GapmeR (F) or in which *LETSI* was overexpressed (G). Vinculin and GAPDH are loading controls. Quantitative data show the abundance of p-SMAD2 relative to t-SMAD2. Data are means  $\pm$  SD from four independent experiments. a.u., arbitrary units. In (B), significance was assessed using two-way ANOVA followed by Tukey's multiple comparisons test. In (C), significance was assessed using one-way ANOVA followed by Dunnett's multiple comparisons test. In (D), significance was assessed using unpaired Student's t test. In (E), significance was assessed by Kolmogorov-Smirnov test. In (F) and (G), significance was assessed using paired Student's t test. \*, 0.01 <  $P$  < 0.05; \*\*, 0.001 <  $P$  < 0.01; \*\*\*, 0.0001 <  $P$  < 0.001; \*\*\*\* $P$  < 0.0001.

Furthermore, we found that *LETSI* promoted the expression of transcripts encoding NR4A1, which potentiates TGF- $\beta$ -SMAD signaling by inhibiting T $\beta$ RI polyubiquitination in breast cancer cells (Fig. 4, C to E; and fig. S5, C and D)<sup>20</sup>. *Cis*-regulation is a mechanism by which nuclear lncRNAs can affect the expression of neighboring genes<sup>41</sup>. However, expression of genes near *LETSI* was not affected by ectopic *LETSI* expression in A549 cells (fig. S8B). This excludes the involvement of *LETSI* in a *cis*-regulatory mechanism.

We next determined whether *LETSI* exerted its function by inducing *NR4A1* expression. Upon *NR4A1* depletion by a selective shRNA or a mixture of four siRNAs, the promotion of TGF- $\beta$ -SMAD3-driven transcriptional response induced by *LETSI* was alleviated in HepG2 cells (Fig. 4F and fig. S5E). Moreover, we demonstrated that *NR4A1* depletion attenuated *LETSI*-mediated promotion of EMT marker expression and migration in A549 cells (Fig. 4, G and H; and fig. S5, F to L). Together, our results suggest that *LETSI* induces *NR4A1* expression to suppress T $\beta$ RI polyubiquitination and enhance TGF- $\beta$ -SMAD signaling, EMT, and migration in cancer cells.

### **NFAT5 interacts with *LETSI*, inhibits T $\beta$ RI polyubiquitination, and potentiates TGF- $\beta$ -induced EMT and cell migration**

To determine whether *LETSI* affected *NR4A1* expression at the transcriptional level, we cloned the 1597-base pair (bp) *NR4A1* promoter [P1; chromosome 12: 52,040,360 to 52,041,947 (GRCh38.p14)] and placed it upstream of a luciferase reporter gene (Fig. 5A). Ectopic *LETSI* expression enhanced transcriptional activity of the *NR4A1* P1 promoter, and further analysis of *NR4A1* promoter truncation mutants suggested that the promoter region containing bps -1238 to -1004 [chromosome 12: 52,040,567 to 52,040,801 (GRCh38.p14)] was required for *LETSI*-driven transcriptional activity (Fig. 5A). Nuclear lncRNAs can participate in gene transcription by interacting with transcription factors or chromatin modifiers<sup>21, 42</sup>. We therefore applied the CRISPR-assisted RNA-protein interaction detection method (CARPID)<sup>43</sup> followed by mass spectrometry to identify nuclear protein partners of *LETSI* (fig. S6A). A well-characterized transcription factor, NFAT5, was enriched as one of the proteins with the highest binding capabilities to *LETSI* (Fig. 5B). We validated the *LETSI*-NFAT5 interaction in the presence or absence of TGF- $\beta$ . Short TGF- $\beta$  stimulation (1 hour) induced a moderate increase in *LETSI* expression (fig. S6B) but potently promoted *LETSI*-NFAT5 interaction (fig. S6C). Moreover,

the interaction between endogenous *LETS1* and endogenous NFAT5 was confirmed using RNA immunoprecipitation (RIP; Fig. 5C and fig. S6D) in MDA-MB-231 cells and between *in vitro*-transcribed *LETS1* and epitope-tagged NFAT5 using RNA pull-down assays in human embryonic kidney (HEK)293T cells (Fig. 5D).

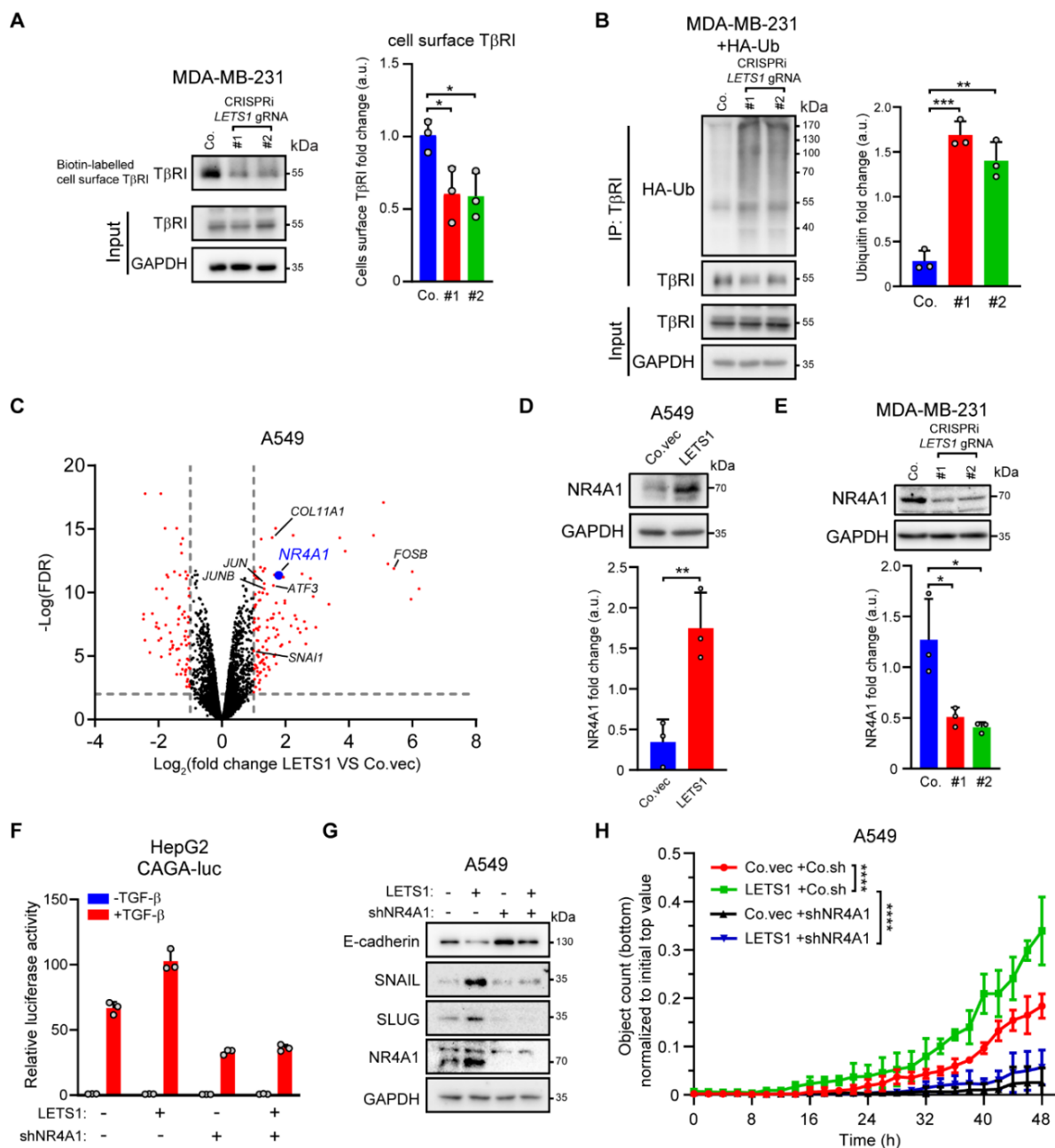


**Fig. 4. *LETS1* inhibits T $\beta$ RI polyubiquitination and promotes T $\beta$ RI stability by inducing NR4A1 expression.** (A) Immunoblotting and quantification of T $\beta$ RI in total cell lysates (input) and biotinylated surface proteins from MDA-MB-231 cells in which *LETS1* was depleted by CRISPRi. Co, empty vector control. GAPDH is a loading control. Results are means  $\pm$  SD from three independent experiments. a.u., arbitrary units. (B) Immunoblotting for HA and T $\beta$ RI in total lysates (input) and T $\beta$ RI immunoprecipitates (IP) from MDA-MB-231 cells expressing HA-ubiquitin (HA-Ub) and empty vector or CRISPRi-gRNAs targeting *LETS1*. Ubiquitin was quantified in the T $\beta$ RI immunoprecipitates. Quantitative data are means  $\pm$  SD from three independent experiments. (C) Volcano plot showing differentially expressed genes (as analyzed by RNA-seq) upon *LETS1* ectopic expression in A549 cells. (D and E) Immunoblotting and quantification of NR4A1 in A549 cells overexpressing *LETS1* (D) and in MDA-MB-231 cells in which *LETS1* was depleted by CRISPRi (E). Co.vec and Co., empty vector controls. Results are means  $\pm$  SD from three independent experiments. (F) Luciferase activity in TGF- $\beta$ -stimulated HepG2 cells transfected with the expression construct for the SMAD3/4 transcriptional reporter CAGA-luc plus the *LETS1* ectopic expression construct and the NR4A1 shRNA construct as indicated. The relative luciferase activities are representative of at

least three independent experiments and expressed as means  $\pm$  SD from three wells of cells per treatment group in one experiment. (G) Immunoblotting for E-cadherin, SNAIL, SLUG, and NR4A1 in A549 cells in which LETS1 was overexpressed and NR4A1 was knocked down as indicated. Blots are representative of at least three independent experiments. (H) Quantification of migrated cells in IncuCyte chemotactic migration assays using A549 cells with LETS1 overexpression and NR4A1 knockdown as indicated. The results are expressed as means  $\pm$  SD from five biological replicates in one independent experiment and representative of three independent experiments. In (A), (B), (D), and (E), significance was assessed using paired Student's t test. In (H), significance was assessed using two-way ANOVA followed by Tukey's multiple comparisons test. \*,  $0.01 < P < 0.05$ ; \*\*,  $0.001 < P < 0.01$ ; \*\*\*,  $0.0001 < P < 0.001$ ; \*\*\*\*  $P < 0.0001$ .

We next investigated the effect of NFAT5 on TGF- $\beta$ -SMAD signaling. Ectopic NFAT5 expression enhanced the TGF- $\beta$ -induced transcriptional response in MCF10A-M2 cells and SMAD2 phosphorylation in MDA-MB-231 cells (Fig. 5, E and F; and fig. S6, E to G). In samples of patients with breast cancer or lung adenocarcinoma, we observed strong positive correlations between *NFAT5* expression and the TGF- $\beta$  gene response signature (fig. S6H). Moreover, *NFAT5* knockdown promoted T $\beta$ RI polyubiquitination in MDA-MB-231 cells (Fig. 5G). Furthermore, NFAT5 enhanced TGF- $\beta$ -induced EMT marker expression and cell migration in MCF10A-M2 cells (Fig. 5, H and I; and fig. S7, A to C). In addition, *NFAT5* expression and *NR4A1* expression showed a positive correlation with the EMT signature in tumor samples from cohorts of patients with breast cancer or lung adenocarcinoma, respectively (fig. S7D).

### ***LETS1* induces NR4A1 expression by cooperating with NFAT5**

Because *LETS1* interacts with NFAT5 and activates *NR4A1* transcription, we hypothesized that NFAT5 was likely to be involved in *LETS1*-induced *NR4A1* expression. As expected, ectopic NFAT5 expression increased *NR4A1* promoter reporter activity in HepG2 cells and *NR4A1* expression in MCF10A-M2 cells (Fig. 6, A to C). Moreover, positive correlations between *NFAT5* and *NR4A1* expression were observed in tumor samples from patients with breast cancer or lung adenocarcinoma (Fig. 6D). To further test whether NFAT5 was required for *LETS1*-mediated *NR4A1* expression, we knocked down *NFAT5* in HepG2 cells ectopically expressing *LETS1*. *LETS1*-induced *NR4A1* promoter activity was attenuated upon *NFAT5* depletion (Fig. 6E). Consistently, *LETS1*-induced *NR4A1* expression was also reduced in MDA-MB-231 cells in which *NFAT5* was knocked down (Fig. 6F). We then analyzed the identified *NR4A1* minimal promoter (P5) sequences and mapped two putative NFAT5-binding sites [chromosome 12: 52,040,615 to 52,040,632 (GRCh38.p14); fig. S8A]. Chromatin IP (ChIP) assays demonstrated strong NFAT5 binding to the *NR4A1* promoter in MDA-MB-231 cells, and ectopic expression of *LETS1* potentiated this (Fig. 6G), indicating that *LETS1* enhances the binding ability of NFAT5 to the *NR4A1* promoter.

### **Discussion**

In this study, we showed that TGF- $\beta$ -SMAD-induced nuclear *LETS1* associated with the transcription factor NFAT5 to facilitate the transcription of *NR4A1*. NR4A1 inhibits T $\beta$ RI polyubiquitination and enhances T $\beta$ RI stability by promoting SMAD7 protein degradation<sup>20</sup>, resulting in an increase in TGF- $\beta$ -SMAD signaling, TGF- $\beta$ -induced EMT, and cancer cell migration and extravasation (Fig. 6H). Thus, we found a previously unidentified mechanism by which TGF- $\beta$ -SMAD signaling is fine-tuned at the receptor level through a specific unannotated lncRNA, *LETS1*. This mechanism is distinct from previous reports of lncRNAs regulating *TBRI* mRNA expression at the transcriptional<sup>30</sup> or posttranscriptional<sup>44-52</sup> level.

The lncRNA *LETS1* promotes TGF- $\beta$ -induced EMT and cancer cell migration by transcriptionally activating a T $\beta$ RI-stabilizing mechanism

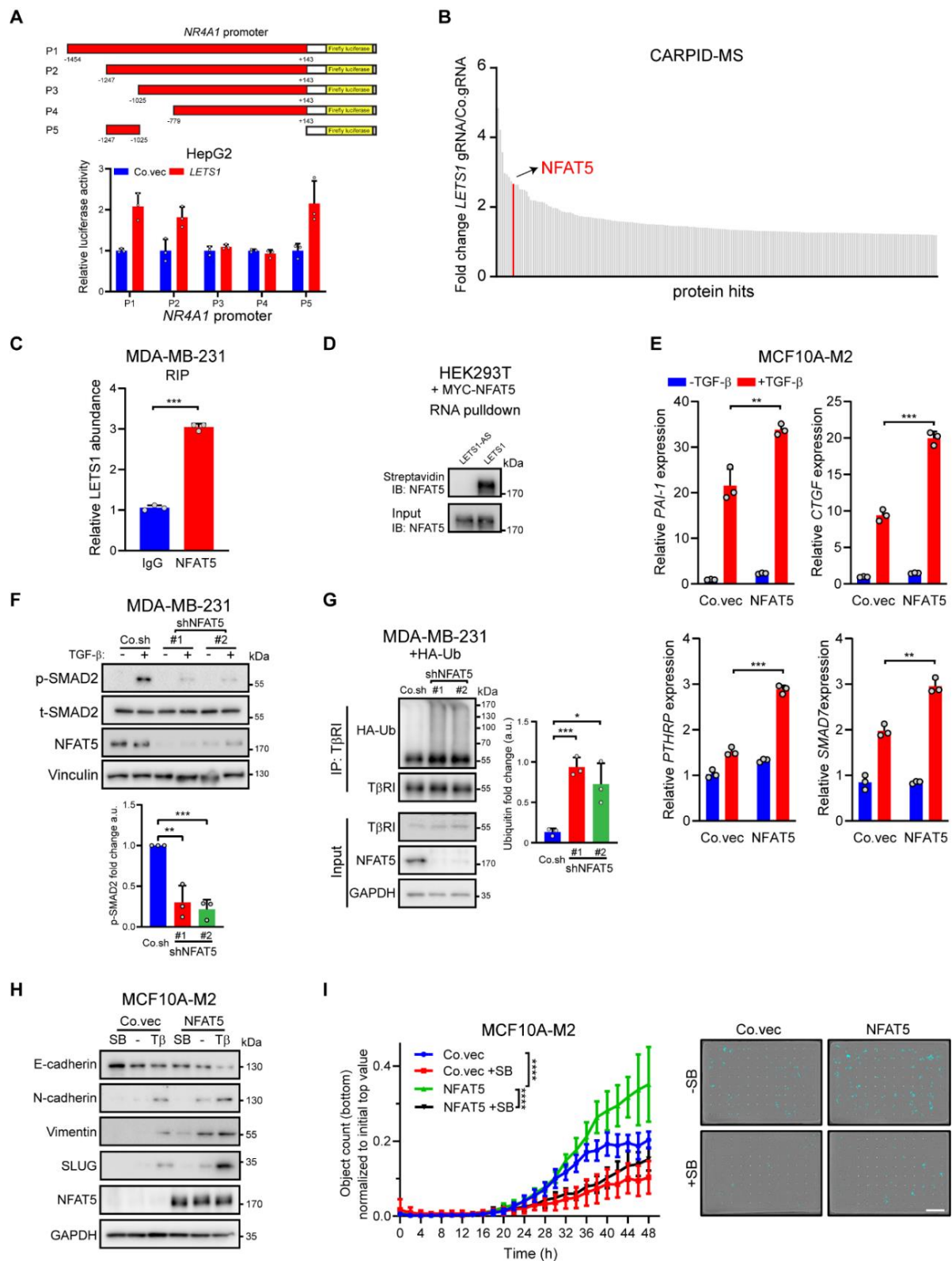


**Fig. 5. NFAT5 interacts with *LETS1*; inhibits T $\beta$ RI polyubiquitination; and potentiates TGF- $\beta$ –SMAD signaling, EMT, and cell migration.** (A) Quantification of luciferase activity in HEPG2 cells coexpressing the indicated *NR4A1* promoter luciferase reporter construct and the *LETS1* ectopic expression construct or empty vector (Co.vec). The relative luciferase activities are representative of at least three independent experiments and expressed as means  $\pm$  SD from three wells of cells per treatment group in one experiment. (B) Proteins that interact with *LETS1* were identified by CARPID followed by mass spectrometry (MS). The top 200 hits are shown, and the bar corresponding to NFAT5 is indicated. (C) RIP assay quantifying *LETS1* abundance in NFAT5 immunoprecipitates from MDA-MB-231 cells. *LETS1* abundance in NFAT5 immunoprecipitates is presented as relative to that in IgG immunoprecipitates. RT-qPCR results are shown as means  $\pm$  SD from three biological

replicates in one independent experiment and representative of at least three independent experiments. (D) Immunoblotting (IB) for NFAT5 in total cell lysates (input) from HEK293T cells expressing MYC-NFAT5 and RNA pull-down assays in which the cell lysates were incubated with biotinylated antisense *LETS1* (*LETS1-AS*) or *LETS1* and affinity-purified with streptavidin beads. Blots are representative of at least three independent experiments. (E) Expression of *PAI-1*, *CTGF*, *PTHRP*, and *SMAD7* in MCF10A-M2 cells overexpressing NFAT5 and stimulated with TGF- $\beta$  or vehicle. RT-qPCR results are shown as means  $\pm$  SD from three biological replicates in one independent experiment and representative of at least three independent experiments. (F) Immunoblotting for p-SMAD2 and t-SMAD2 and NFAT5 in TGF- $\beta$ -stimulated MDA-MB-231 cells in which *NFAT5* was knocked down by two independent shRNAs. Quantitative data show the abundance of p-SMAD2 relative to t-SMAD2. Vinculin is a loading control. Results are means  $\pm$  SD from three independent experiments. a.u., arbitrary units. (G) Immunoblotting for HA and T $\beta$ RI in total lysates (input) and T $\beta$ RI immunoprecipitates (IP) from MDA-MB-231 cells expressing HA-Ub and transfected with empty vector (Co.sh) or *NFAT5*-targeting shRNA. Ubiquitin was quantified in the T $\beta$ RI immunoprecipitates. GAPDH is a loading control. Results are means  $\pm$  SD from three independent experiments. (H) Immunoblotting for E-cadherin, N-cadherin, Vimentin, SLUG, and NFAT5 in MCF10A-M2 cells overexpressing NFAT5 or empty vector and treated with vehicle (-), SB431542 (SB), or TGF- $\beta$  (T $\beta$ ). Blots are representative of at least three independent experiments. (I) Quantification of migrated cells in IncuCyte chemotactic migration assays using MCF10A-M2 cells overexpressing NFAT5 and treated with SB431542 or vehicle. The cells that migrated to the bottom chambers are marked in blue in the images. The migration results are expressed as means  $\pm$  SD from 12 biological replicates in one independent experiment and representative of at least three independent experiments. Scale bar, 400  $\mu$ m. In (C) and (E), significance was assessed using unpaired Student's t test. In (F) and (G), significance was assessed using paired Student's t test. In (I), significance was assessed using two-way ANOVA followed by Tukey's multiple comparisons test. \*, 0.01 < *P* < 0.05; \*\*, 0.001 < *P* < 0.01; \*\*\*, 0.0001 < *P* < 0.001; \*\*\*\* *P* < 0.0001.

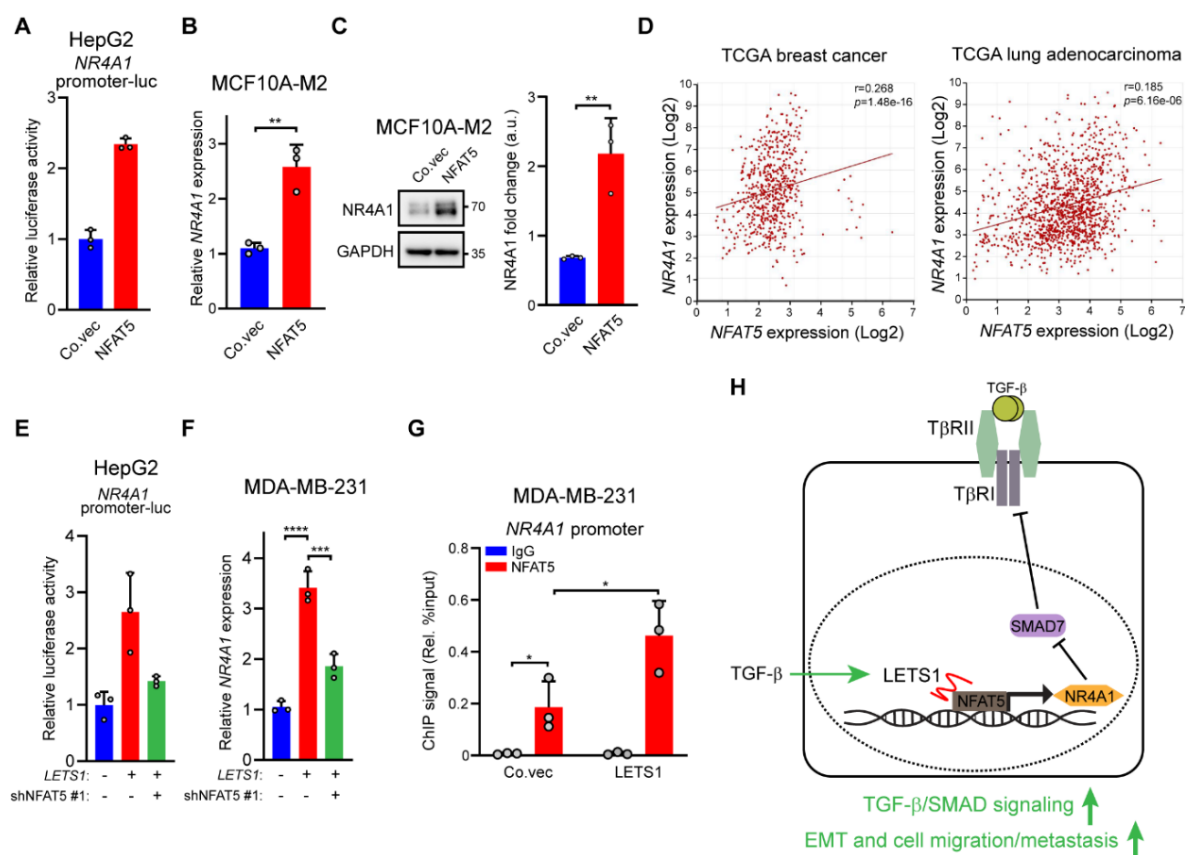


**Fig. 6. *LETS1* cooperates with NFAT5 to induce *NR4A1* expression.** (A) Quantification of luciferase activity in HepG2 cells coexpressing the *NR4A1* promoter luciferase reporter P5 and the NFAT5 expression construct or empty vector (Co.vec). The relative luciferase activities are representative of at least three independent experiments and expressed as means  $\pm$  SD from three wells of cells per treatment group in one experiment. (B) *NR4A1* expression in MCF10A-M2 cells transfected with the NFAT5 expression construct or empty vector. RT-qPCR results are shown as means  $\pm$  SD from three biological replicates in one independent experiment and representative of at least three independent experiments. (C) Immunoblotting for NR4A1 in MCF10A-M2 cells overexpressing NFAT5 or transfected with empty vector. GAPDH is a loading control. Results are means  $\pm$  SD from three independent experiments. a.u., arbitrary units. (D) Correlations between *NFAT5* and *NR4A1* expression in samples of patients with breast cancer or lung adenocarcinoma. (E) Quantification of *NR4A1* promoters luciferase reporter activity in HepG2 cells transfected with the *LETS1* expression construct and the shNFAT5 no. 1 construct as indicated. The relative luciferase activities are representative of at least three independent experiments and expressed as means  $\pm$  SD from three wells of cells per treatment group in one experiment. (F) Quantification of *NR4A1* expression in MDA-MB-231 cells expressing the *LETS1* expression construct and the shNFAT5 no. 1 construct as indicated. RT-qPCR results are shown as means

## The lncRNA *LETS1* promotes TGF- $\beta$ -induced EMT and cancer cell migration by transcriptionally activating a T $\beta$ RI-stabilizing mechanism

$\pm$  SD from three biological replicates in one independent experiment and representative of at least three independent experiments. (G) ChIP analysis of the *NR4A1* promoter region in MDA-MB-231 cells transduced with the *LETS1* expression construct or empty vector. IgG was included as the control for IP. RT-qPCR results are shown as means  $\pm$  SD from three independent experiments. (H) Schematic model of the action of *LETS1* on TGF- $\beta$ -SMAD signal transduction through the potentiation of NFAT5-mediated *NR4A1* transcription. In (B), significance was assessed using unpaired Student's t test. In (C) and (G), significance was assessed using paired Student's t test. In (D), the statistical analysis was performed using Pearson's correlation ( $r$ ) test. In (F), significance was assessed using one-way ANOVA followed by Dunnett's multiple comparisons test. \*,  $0.01 < P < 0.05$ ; \*\*,  $0.001 < P < 0.01$ ; \*\*\*,  $0.0001 < P < 0.001$ ; \*\*\*\*  $P < 0.0001$ .

The pivotal promoting effects of *LETS1* on TGF- $\beta$ -SMAD signaling and on TGF- $\beta$ -induced EMT and migration were shown in our study by multiple orthogonal approaches, including GapmeRs, CRISPRi, CRISPR-CasRx, and ectopic expression to manipulate *LETS1* expression. Moreover, possible shortcomings with each approach were as much as possible controlled for. For example, off-target effects of *LETS1* targeting by CRISPRi<sup>53</sup> on neighboring gene expression were excluded (fig. S8B). Results of *LETS1* misexpression were shown in multiple cell lines, and *in vitro* cell culture studies were complemented with experiments using the *in vivo* zebrafish embryo xenograft model for extravasation. Conservation of the lncRNA sequence is much lower than that of protein-coding RNAs among vertebrates<sup>54</sup>. However, lncRNA orthologs with similar secondary or tertiary structures but diverse sequences may exert the same functions in different species<sup>55</sup>. We performed a sequence similarity search for *LETS1* in the mouse transcriptome, but no ortholog of *LETS1* was identified, making genetic analysis of *LETS1* function in mouse cancer models challenging.

Cell surface T $\beta$ RI is highly dynamic and undergoes rapid degradation after being polyubiquitinated by E3 ligases such as SMURF2 and NEDD4<sup>56, 57</sup>. As an adaptor of T $\beta$ RI and E3 ligase interactions, SMAD7 potentiates the E3 ligase-mediated polyubiquitination of T $\beta$ RI<sup>56, 57</sup>. NR4A1 potentiates TGF- $\beta$ -SMAD signaling by enhancing SMAD7 degradation in breast and lung cancer cells<sup>20, 58, 59</sup>. Our results showed that *NR4A1* knockdown greatly mitigated the promoting effects of *LETS1* on TGF- $\beta$  signaling, TGF- $\beta$ -induced EMT, and cell migration, suggesting that NR4A1 is a major *LETS1* downstream effector. However, because the expression of multiple genes was altered upon ectopic *LETS1* expression in our transcriptome analysis, other genes also likely participate in the effects mediated by *LETS1*.

NFAT5 was identified as a protein partner of *LETS1*, and TGF- $\beta$  stimulation potently promoted *LETS1*-NFAT5 interaction in MDA-MB-231 cells. A possible explanation for this result could be that TGF- $\beta$  treatment alters the chemical modification (such as N6-methyladenosine) of *LETS1* and/or posttranslational modification (such as phosphorylation) of NFAT5, thereby promoting this interaction. Therefore, further investigation is required to explore these and other possibilities.

We showed that NFAT5 directly bound to the *NR4A1* promoter and stimulated its activity, which was strengthened upon *LETS1* ectopic expression. Previous reports have documented that the promoter activity of *NR4A1* can be enhanced by the transcription factor CCAAT/enhancer binding protein  $\beta$  (C/EBP $\beta$ ) and several lysine methyltransferases that are recruited by *LnclY6C*<sup>60</sup>. Compared with other NFAT member proteins, NFAT5 lacks the structural domain that mediates the cooperative complex formation with other transcription factors<sup>61, 62</sup>. It is possible that the interaction with *LETS1* may provide extra docking sites on NFAT5 for other proteins to potentiate NFAT5 transcriptional activity or for chromatin modifiers to change the local chromatin status. In addition, the C-terminal dimerization of NFAT5 is required for its DNA binding activity<sup>63</sup>. *LETS1* may facilitate the formation of NFAT5 homodimers or stabilize the dimeric complex through its binding to NFAT5. Because the affinity of NFAT5 for DNA is much lower than that of other NFAT family members<sup>61</sup>,

another possibility is that the interaction with *LETS1* may change the conformation of NFAT5 toward a status with stronger DNA binding ability. However, whether the contribution of *LETS1* to NFAT5-mediated transcription is confined to a certain subset of target genes including *NR4A1* or this effect can be expanded to general transcriptional events directed by NFAT5 requires further investigation.

Our results showed that NFAT5 is a positive regulator of TGF- $\beta$ -induced EMT and cell migration in breast and lung cancer cells. These results are consistent with other studies demonstrating the tumor-promoting role of NFAT5 through the induction of the expression of genes encoding proteins such as aquaporin-5 and S100 calcium binding protein A4<sup>64–67</sup>. We found that TGF- $\beta$ -SMAD signaling was required for NFAT5 to induce EMT and migration in cell culture models and observed strong correlations between *NFAT5* expression and the TGF- $\beta$  response gene signature or the EMT signature in RNA profiles obtained from biopsies of patients with breast cancer or lung adenocarcinoma. These results reveal a previously undescribed mechanism by which NFAT5 promotes cancer progression and highlight the therapeutic potential of targeting NFAT5 in cancer. Compared with enzymes and kinases, transcription factors are difficult to target with small-molecule inhibitors because of the lack of active sites or allosteric regulatory pockets<sup>68</sup>. DNA-based proteolysis targeting chimera (PROTAC) approaches such as transcription factor (TF)-PROTAC<sup>69</sup> and oligonucleotide-based PROTAC<sup>70</sup> have been developed to selectively and efficiently degrade transcription factors of interest. Therefore, on the basis of the consensus DNA binding sequence of NFAT5, NFAT5-specific DNA oligomers could be designed and combined with the E3 ligase ligands typically used for TF-PROTAC to target NFAT5 for degradation in cancer cells.

In conclusion, we identified *LETS1* as a potent activator of TGF- $\beta$ -induced EMT and cancer cell migration and extravasation, all of which contribute to cancer progression, by promoting T $\beta$ RI cell surface abundance. Inhibition of *LETS1* expression, for example, using GapmeR<sup>71</sup> or ribonuclease-targeting chimera (RIBOTAC)<sup>72</sup> approaches, may therefore have therapeutic potential in cancer.

## Materials and methods

### Cell culture and reagents

HEK293T (CRL-1573), HepG2 (HB-8065), A549 (CRM-CCL-185), and MDA-MB-231 (CRM-HTB-26) cells were purchased from the American Type Culture Collection. MCF10A-M1 and MCF10A-M2 cells were provided by F. Miller (Barbara Ann Karmanos Cancer Institute, Detroit, USA). All the cell lines were cultured as described previously<sup>73</sup>. Recombinant TGF- $\beta$ 3 was a gift from A. P. Hinck (University of Pittsburgh). Cells were frequently tested for absence of mycoplasma, and cell lines were authenticated by short tandem repeat profiling.

### Plasmid construction

*LETS1* cDNA was cloned from A549 cells and ligated to the pCDH-EF1 $\alpha$ -MCS-polyA-PURO lentiviral vector. Guide RNAs (gRNAs) for CRISPRi and CRISPR-CasRx were inserted into the pLKO.1-U6-PURO (AA19) and pRX004-pregRNA (Addgene, 109054), respectively. *NR4A1* promoter fragments were cloned into the pGL4-luc backbone (Promega). The primers used for molecular cloning are listed in table S1.

### Lentiviral transduction and transfection

Production of lentivirus was described elsewhere<sup>73</sup>. Cells stably expressing the indicated constructs were selected by adding the corresponding antibiotics to the culture medium after 2

days postinfection. We used TRCN0000010477 (no. 1) and TRCN0000010478 (no. 2) for *SMAD2* knockdown, TRCN0000330128 (no. 1) and TRCN0000330127 (no. 2) for *SMAD3* knockdown, TRCN0000040031 for *SMAD4* knockdown, TRCN0000019426 for *NR4A1* knockdown, and TRCN0000020019 (no. 1) and TRCN0000020021 (no. 2) for *NFAT5* knockdown. For the transfection of GapmeRs (Eurogentec) and *NR4A1*-targeting SMARTpool siRNA (Horizon, L-003426),  $1.2 \times 10^5$  A549 cells were seeded in wells of a 12-well plate and incubated with complex formed by Lipofectamine 3000 (Thermo Fisher Scientific, L3000015) and GapmeRs (25 nM) or siRNA (25 nM). Knockdown efficiency was quantified at 2 days after transfection. The sequences of GapmeRs are listed in table S2.

### RT-qPCR

To check *LETS1* expression upon TGF- $\beta$  stimulation, cells were starved for 16 hours and treated with vehicle control or TGF- $\beta$  (5 ng/ $\mu$ l) for indicated durations as indicated in the panels or 4 hours, if the treatment duration is not specified. CHX (50  $\mu$ g/ml) was used to pretreat MDA-MB-231 cells for 30 min before adding TGF- $\beta$  or vehicle. To evaluate TGF- $\beta$ -induced target gene expression, cells were starved for 16 hours and treated with vehicle control or TGF- $\beta$  (1 ng/ $\mu$ l) for 4 hours. RNA extraction and RT-qPCR were performed as described previously<sup>73</sup>. Expression of target genes was normalized to GAPDH. The primer sequences used for RT-qPCR are listed in table S3.

### Western blotting

To detect EMT marker expression, A549 or MCF10A-M2 cells were treated with TGF- $\beta$  (1 ng/ml for A549 and 5 ng/ml for MCF10A-M2, respectively) or vehicle for 1 (A549) or 3 days (MCF10A-M2). To check TGF- $\beta$ -induced p-SMAD2, TGF- $\beta$  (1 ng/ml) or vehicle was added for indicated time points or 1 hour, if the treatment duration is not specified. Western blotting was performed as described previously<sup>73</sup>. The primary antibodies are listed in table S4.

### Coding potential prediction

CPAT software was used to predict the coding potential of protein-coding mRNAs or lncRNAs as described elsewhere<sup>37</sup>.

### Transcriptional reporter assays

Reporter assays were performed as described previously<sup>73</sup> to quantify SMAD3/4-driven transcriptional CAGA-luc reporter activity in HepG2 cells. Cells were serum-starved for 6 hours and stimulated with TGF- $\beta$  (1 ng/ml) or vehicle control for 16 hours. To measure *NR4A1* promoter fragment activity, 320 ng of the *LETS1* or *NFAT5* expression construct, 100 ng of the *NR4A1* promoter luciferase reporter, and 80 ng of the  $\beta$ -galactosidase expression construct were cotransfected into HepG2 cells using polyethyleneimine (Polysciences, 23966). Luciferase activity was measured with the substrate d-luciferin (Promega) and a luminometer (PerkinElmer) and normalized to  $\beta$ -galactosidase activity.

### Fluorescent staining

To evaluate the expression and localization of F-actin, fluorescent staining was performed as previously described<sup>74, 75</sup>. Briefly, A549 cells were stimulated with SB431542 (SB; 10  $\mu$ M) or TGF- $\beta$  (1 ng/ml) or the corresponding vehicle for 48 hours. The fixed cells were stained with phalloidin conjugated with Alexa Fluor 488 (1:500 dilution; Thermo Fisher Scientific, A12379) for 30 min at room temperature. VECTASHIELD Antifade Mounting Medium with DAPI (4',6-diamidino-2-phenylindole; Vector Laboratories, H-1200) was used to mount coverslips. A Leica SP8 confocal microscope (Leica Microsystems) was used to acquire images. Quantification of average F-actin intensity was performed using the ImageJ software.



### **Ubiquitination assay**

Ubiquitination assay was performed as previously described<sup>73</sup> in MDA-MB-231 cells stably expressing hemagglutinin (HA)-ubiquitin.

### **Chemotactic migration and live-cell imaging using IncuCyte**

An IncuCyte live-cell imaging system (Essen BioScience) was used to monitor cell chemotactic migration as previously described<sup>73</sup>. Cells were treated with TGF- $\beta$  (5 ng/ml) or vehicle during the assay. To quantify the dynamic GFP signal in A549 cells,  $5 \times 10^3$  A549 cells with SMAD3/4-driven GFP expression<sup>39</sup> were seeded in a 96-well plate. Cells were serum-starved for 16 hours and stimulated with TGF- $\beta$  (1 ng/ml) or vehicle, and the real-time green integrated intensity was monitored using the IncuCyte system<sup>39</sup>.

### **Subcellular fractionation**

In brief, cell pellets were lysed in buffer A [50 mM Tris-HCl (pH 7.4), 150 mM NaCl, 1% NP-40, and 0.25% sodium deoxycholate] for 15 min on ice. The supernatant was collected as the cytoplasmic fraction after centrifugation at 3000g for 5 min. Phosphate-buffered saline (PBS) was used to wash the pellet, which was then resuspended in buffer B [50 mM Tris-HCl (pH 7.4), 400 mM NaCl, 1% NP-40, 0.5% sodium deoxycholate, and 1% SD]. The supernatant was collected as the nuclear fraction after 20 min of incubation on ice and centrifugation at 12,000g for 15 min.

### **RACE**

RACE was carried out on A549 cells using a SMARTer RACE 5' /3' Kit (TaKaRa, 634859). 5' /3' RACE products were cloned and transformed into competent cells, and 20 independent colonies were picked for Sanger sequencing.

### **RIP**

RIP was performed using a Magna RIP RNA-Binding Protein IP Kit (Merck Millipore, 17-700). A total of 2.5  $\mu$ g of an anti-NFAT5 antibody (Thermo Fisher Scientific, PA1-023) or normal rabbit immunoglobulin G (IgG) were added to the cell lysates. To lower the background, we optimized the supplied instructions by adding a bead-blocking step. The magna beads were blocked with 5  $\mu$ l of yeast tRNA (Invitrogen, AM7119) and 5  $\mu$ l of bovine serum albumin (Invitrogen, AM2618) for 2 hours at 4°C before being used for IP.

### **RNA pull-down assay**

A MEGAscript Kit (Thermo Fisher Scientific, AM1334) was used to in vitro transcribe antisense and sense *LETS1*, which were then biotinylated with an RNA 3' End Desthiobiotinylation Kit (Thermo Fisher Scientific, 20160). RNA pull-down assays were performed using a Magnetic RNA-Protein Pull-Down Kit (Thermo Fisher Scientific, 20164). NFAT5 expression was analyzed by Western blotting.

### **ChIP assay**

Briefly,  $1 \times 10^7$  MDA-MB-231 cells were cross-linked with 1% formaldehyde for 10 min and resuspended in lysis buffer [5 mM Pipes (pH 8.0), 85 mM KCl, and 0.5% NP-40] for 10 min on ice. After centrifugation at 500g for 5 min at 4°C, the pellet was lysed in nuclear lysis buffer [50 mM Tris-HCl (pH 8), 10 mM EDTA, and 1% SD] for 10 min on ice. Afterwards, the chromatin was sheared using a sonicator (Diagenode) at 30% amplitude for 3 min. After centrifugation at 12,000g for 30 min at 4°C, the supernatant was diluted five times with IP dilution buffer [50 mM Tris-HCl (pH 7.5), 150 mM NaCl, 1 mM EDTA, 1% NP-40, and 0.25% sodium deoxycholate]. Protein A Sepharose beads (GE Healthcare, catalog no. 17-0963-03)

and the salmon sperm DNA were used to preclear the cell lysates for 1 hour at 4°C. Subsequently, the cell lysates were incubated with 10  $\mu$ g of IgG (Cell Signaling Technology, 2729) or anti-NFAT5 antibody (Thermo Fisher Scientific, PA1-023) overnight at 4°C. The next day, 20  $\mu$ g of Protein A Sepharose beads were added to the cell lysates and incubated for 2 hours at 4°C. After five times washing, the beads were treated with ribonuclease A and proteinase K, and the DNA was extracted by isopropanol. The amount of precipitated *NR4A1* promoter region was analyzed by RT-qPCR and the absolute quantification method.

### **CARPID and mass spectrometry**

MDA-MB-231 cells stably expressing TurboID-dCasRx and CRISPR-CasRx gRNA was treated with TGF- $\beta$  (2.5 ng/ml) or vehicle for 1 hour. Two hundred  $\mu$ M biotin (Sigma-Aldrich, B4639) dissolved in medium was used to activate biotinylation in cells cultured in a 15-cm dish for 30 min. Cells were washed with cold PBS twice and suspended with 600  $\mu$ l of lysis buffer [50 mM Tris-HCl (pH 7.4), 500 mM NaCl, 0.4% SD, 5 mM EDTA, H<sub>2</sub>O, and 1 mM dithiothreitol]. After mixing with 240  $\mu$ l of 20% Triton X-100, cell lysates were sonicated at 80% amplitude for 10 s four times. The supernatant was collected after centrifugation at 12,000g for 30 min at 4°C and added with 1 ml of 50 mM Tris-HCl (pH 7.5). Twenty-five microliters of Streptavidin Agarose beads (Millipore, 69203) were added to the supernatant and incubated on a rotator overnight at 4°C. After washing with wash buffer 1 (2% SD), wash buffer 2 [0.1% deoxycholate, 1% Triton X-100, 500 mM NaCl, 1 mM EDTA, and 50 mM Hepes (pH 7.5)], wash buffer 3 [250 mM LiCl, 0.5% Triton X-100, 0.5% deoxycholate, 1 mM EDTA, and 10 mM Tris-HCl (pH 8.1)], wash buffer 4 [50 mM Tris-HCl (pH 7.4) and 50 mM NaCl], and 50 mM ammonium bicarbonate three times, the beads were boiled for 5 min in sample buffer, and biotinylated proteins of interest were analyzed by Western blotting. For mass spectrometry analysis, the beads were resuspended in 250  $\mu$ l of 50 mM ammonium bicarbonate and incubated with 250 ng of trypsin (Promega, V5280) overnight at 37°C. The beads were separated with a prewashed 0.4- $\mu$ m filter (Millipore, UFC30HV00). Digested peptides were desalted using StageTips<sup>76</sup> and analyzed as in<sup>77</sup>. Briefly, samples were measured in an Orbitrap Exploris 480 (Thermo Fisher Scientific) mass spectrometer coupled to an Ultimate 3000 Ultra-High-Performance Liquid Chromatography (Dionex). Digested peptides were separated using a 50-cm-long fused silica emitter (FS360-75-15-N-5-C50, New Objective, MA, USA) in-house packed with 1.9- $\mu$ m C18-AQ beads (Reprospher-DE, Pur, Dr. Maisch, Ammerburch-Entringen, Germany) and heated to 50°C in a Column Oven for electrospray ionization/Nanospray (Sonation, Germany). Peptides were separated by liquid chromatography using a gradient from 2 to 32% acetonitrile with 0.1% formic acid for 60 min, followed by column reconditioning for 25 min. A lock mass of 445.12003 (polysiloxane) was used for internal calibration. Data were acquired in a data-dependent acquisition mode with a TopSpeed method with cycle time of 3 s with a scan range of 350 to 1600 mass/charge ratio (m/z) and resolutions of 60,000 and 30,000 for MS1 and MS2, respectively. For MS2, an isolation window of 1.2 m/z and a higher-energy C-trap dissociation (HCD) collision energy of 30% were applied. Precursors with a charge of 1 and higher than 6 were excluded from triggering MS2 as well as previously analyzed precursors with a dynamic exclusion window of 30 s.

### **Mass spectrometry data analysis**

Mass spectrometry data were analyzed using MaxQuant v2.1.3.0 according to Tyanova et al.<sup>78</sup> with the following modifications: Maximum missed cleavages by trypsin was set to 3. Searches were performed against an in silico-digested database from the human proteome including isoforms and canonical proteins (UniProt, 29 August 2022). Oxidation (M), acetyl (protein N-terminal), were set as variable modifications with a maximum of 3. Carbamidomethyl (C) was disabled as a fixed modification. Label-free quantification was activated not enabling fast label-

free quantification (LFQ). The match between runs feature was activated with default parameters.

MaxQuant output data were further processed in the Perseus Computational Platform v1.6.14.0 according to Tyanova et al.<sup>79</sup>. LFQ intensity values were log<sub>2</sub>-transformed, and potential contaminants and proteins identified by site only or reverse peptide were removed. Samples were grouped in experimental categories, and proteins not identified in three of three replicates in at least one group were also removed. Missing values were imputed using normally distributed values with a 2.1 downshift (log<sub>2</sub>) and a randomized 0.1 width (log<sub>2</sub>) considering whole-matrix values. Two-sided t tests were performed to compare groups. Analyzed data were exported from Perseus and further processed in Microsoft Excel 365 for comprehensive visualization. Protein hits were ranked on the basis of the fold change between two *LETS1*-targeting gRNAs and the control gRNA expression vector (Co.gRNA).

### **Transcriptional profiling and GSEA**

To identify TGF- $\beta$ -induced lncRNAs, cells were serum-starved overnight and stimulated without (0 hours) or with TGF- $\beta$  (5 ng/ml) for 2, 8, and 24 hours. RNA was extracted using TRIzol reagent (Thermo Fisher Scientific, 15596026). Libraries were then constructed, and RNA sequencing (RNA-seq) was performed on an Illumina HiSeq [Beijing Genomics Institute (BGI), Shenzhen]. Differentially expressed lncRNAs were analyzed by BGI. To identify mRNAs affected by *LETS1*, we generated A549 cells stably expressing *LETS1*. The DNBSeg platform (BGI, Hong Kong) was used to perform RNA-seq. Analysis of differentially expressed genes was performed as described previously<sup>73</sup>. The correlations between *LETS1* and TGF- $\beta$ /SMAD signaling and EMT were performed with the GSEA software<sup>80</sup> using the TGF- $\beta$  (TGFB\_UP.V1\_UP) gene response signature<sup>40</sup> and the EMT (GOBP\_EPITHELIAL\_TO\_MESENCHYMAL\_TRANSITION; Gene Ontology: 0001837) gene signature as inputs.

### **Gene correlation analysis in databases**

Correlations between *NFAT5* and *NR4A1* expression or between *NFAT5* expression and the TGF- $\beta$  gene response signature or the EMT gene signature were performed in the breast (R2 internal identifier: ps\_avgpres\_tcgabrcav32a1221\_gencode36) and lung (R2 internal identifier: ps\_avgpres\_tcgaluadv32a589\_gencode36) cohorts of patients with cancer in the R2: Genomics Analysis and Visualization Platform (<http://r2.amc.nl>).

### **In situ hybridization staining**

MDA-MB-231 cells were transfected with a scrambled GapmeR or *LETS1*-targeting GapmeR no. 1 and stimulated with TGF- $\beta$  (5 ng/ml) or vehicle for 2 hours. The expression and localization of *LETS1* were detected by an RNAScope Multiplex Fluorescent kit (Advanced Cell Diagnostics, 323100) and an *in situ* probe for *LETS1* (Advanced Cell Diagnostics, 840831). A DMi8 inverted fluorescence microscope (Leica) was used to acquire images.

### **Embryonic zebrafish cancer cell extravasation assay**

The experiments were conducted in a licensed establishment for the breeding and use of experimental animals [Leiden University (LU)] and subject to internal regulations and guidelines, stating that advice was taken from the Animal Welfare Body to minimize suffering for all experimental animals housed at the facility. The zebrafish assays described are not considered as an animal experiment under the Experiments on Animals Act (Wod, effective 2014), the applicable legislation in the Netherlands in accordance with the European guidelines (EU directive no. 2010/63/EU) regarding the protection of animals used for scientific purposes. Therefore, a license specific for these assays on zebrafish larvae (<5 days) was not required.

MDA-MB-231 or A549 cells labeled with mCherry were injected into the ducts of Cuvier of embryos from transgenic zebrafish [fli; enhanced GFP (EGFP)] as previously described<sup>81</sup>. Zebrafish embryos were maintained in 33°C egg water for 5 days. To check the effect of TGF- $\beta$  signaling blockage on cell extravasation, SB431542 (SB; 1  $\mu$ M) or vehicle was added to egg water during the assay. Zebrafish were fixed with 4% formaldehyde. An inverted SP5 stimulated emission depletion (STED) confocal microscope (Leica) was used to visualize zebrafish embryos and injected cancer cells. At least 30 embryos per group were quantified. Two independent experiments were performed, and representative results are shown.

### Statistical analysis

Statistical analysis was performed using GraphPad Prism 9.3.1. All measurements in this study were taken from distinct samples.

### References

1. Pastushenko, I. & Blanpain, C. EMT transition states during tumor progression and metastasis. *Trends Cell Biol.* **29**, 212-226 (2019).
2. Gui, P.L. & Bivona, T.G. Evolution of metastasis: new tools and insights. *Trends Cancer* **8**, 98-109 (2022).
3. Hanahan, D. Hallmarks of Cancer: New Dimensions. *Cancer Discov.* **12**, 31-46 (2022).
4. Yang, J. *et al.* Guidelines and definitions for research on epithelial-mesenchymal transition. *Nat. Rev. Mol. Cell Biol.* **21**, 341-352 (2020).
5. Sha, Y.T. *et al.* Intermediate cell states in epithelial-to-mesenchymal transition. *Phys. Biol.* **16** (2019).
6. Hendrix, M.J.C., Seftor, E.A., Seftor, R.E.B. & Trevor, K.T. Experimental co-expression of vimentin and keratin intermediate filaments in human breast cancer cells results in phenotypic interconversion and increased invasive behavior. *Am. J. Pathol.* **150**, 483-495 (1997).
7. Schliekelman, M.J. *et al.* Molecular portraits of epithelial, mesenchymal, and hybrid states in lung adenocarcinoma and their relevance to survival. *Cancer Res.* **75**, 1789-1800 (2015).
8. Dmello, C. *et al.* Vimentin regulates differentiation switch via modulation of keratin 14 levels and their expression together correlates with poor prognosis in oral cancer patients. *Plos One* **12**, e0172559 (2017).
9. George, J.T., Jolly, M.K., Xu, S., Somarelli, J.A. & Levine, H. Survival outcomes in cancer patients predicted by a partial EMT gene expression scoring metric. *Cancer Res.* **77**, 6415-6428 (2017).
10. Grosse-Wilde, A. *et al.* Stemness of the hybrid epithelial/mesenchymal state in breast cancer and its association with poor survival. *Plos One* **10**, e0126522 (2015).
11. Hao, Y., Baker, D. & ten Dijke, P. TGF- $\beta$ -mediated epithelial-mesenchymal transition and cancer metastasis. *Int. J. Mol. Sci.* **20**, 2767 (2019).
12. Fan, C., Zhang, J., Hua, W. & ten Dijke, P. Biphasic role of TGF- $\beta$  in cancer progression: From tumor suppressor to tumor promotor. *Reference Module in Biomed. Sci.*, (2018).
13. Tzavlaki, K. & Moustakas, A. TGF- $\beta$  signaling. *Biomolecules* **10**, 487 (2020).
14. Hata, A. & Chen, Y.G. TGF- $\beta$  signaling from receptors to SMADs. *Cold Spring Harb. Perspect. Biol.* **8**, a022061 (2016).
15. Yan, X., Xiong, X. & Chen, Y.G. Feedback regulation of TGF- $\beta$  signaling. *Acta Biochim. Biophys. Sin.* **50**, 37-50 (2018).
16. Budi, E.H., Duan, D. & Derynck, R. Transforming growth factor- $\beta$  receptors and SMADs: Regulatory complexity and functional versatility. *Trends Cell Biol.* **27**, 658-672 (2017).
17. Kavsak, P. *et al.* SMAD7 binds to Smurf2 to form an E3 ubiquitin ligase that targets the TGF $\beta$  receptor for degradation. *Mol. Cell* **6**, 1365-1375 (2000).
18. Koinuma, D. *et al.* Arkadia amplifies TGF- $\beta$  superfamily signalling through degradation of SMAD7. *EMBO J.* **22**, 6458-6470 (2003).
19. Zhang, L. *et al.* RNF12 controls embryonic stem cell fate and morphogenesis in zebrafish embryos by targeting SMAD7 for degradation. *Mol. Cell* **46**, 650-661 (2012).
20. Zhou, F. *et al.* Nuclear receptor NR4A1 promotes breast cancer invasion and metastasis by activating TGF- $\beta$  signalling. *Nat. Commun.* **5**, 3388 (2014).
21. Statello, L., Guo, C.J., Chen, L.L. & Huarte, M. Gene regulation by long non-coding RNAs and its biological functions. *Nat. Rev. Mol. Cell Biol.* **22**, 96-118 (2021).
22. Nandwani, A., Rathore, S. & Datta, M. LncRNAs in cancer: Regulatory and therapeutic implications. *Cancer Lett.* **501**, 162-171 (2021).
23. Lin, C. & Yang, L. Long noncoding RNA in cancer: Wiring signaling circuitry. *Trends Cell Biol.* **28**, 287-301 (2018).

24. Mattick, J.S. & Rinn, J.L. Discovery and annotation of long noncoding RNAs. *Nat. Struct. Mol. Biol.* **22**, 5–7 (2015).
25. Palazzo, A.F. & Koonin, E.V. Functional long non-coding RNAs evolve from junk transcripts. *Cell* **183**, 1151–1161 (2020).
26. Tay, Y., Rinn, J. & Pandolfi, P.P. The multilayered complexity of ceRNA crosstalk and competition. *Nature* **505**, 344–352 (2014).
27. Thomson, D.W. & Dinger, M.E. Endogenous microRNA sponges: Evidence and controversy. *Nat. Rev. Genet.* **17**, 272–283 (2016).
28. Yuan, J.H. *et al.* A long noncoding RNA activated by TGF- $\beta$  promotes the invasion-metastasis cascade in hepatocellular carcinoma. *Cancer Cell* **25**, 666–681 (2014).
29. Richards, E.J. *et al.* Long non-coding RNAs (LncRNA) regulated by transforming growth factor (TGF)  $\beta$ : LncRNA-hit-mediated TGF $\beta$ -induced epithelial to mesenchymal transition in mammary epithelia. *J. Biol. Chem.* **290**, 6857–6867 (2015).
30. Xu, L. *et al.* Long non-coding RNA SMASR inhibits the EMT by negatively regulating TGF- $\beta$ /SMAD signaling pathway in lung cancer. *Oncogene* **40**, 3578–3592 (2021).
31. Sakai, S. *et al.* Long noncoding RNA ELIT-1 acts as a SMAD3 cofactor to facilitate TGF- $\beta$ /SMAD signaling and promote epithelial-mesenchymal transition. *Cancer Res.* **79**, 2821–2838 (2019).
32. Papoutsoglou, P. *et al.* The TGFB2-AS1 lncRNA regulates TGF- $\beta$  signaling by modulating corepressor activity. *Cell Rep.* **28**, 3182–3198.e11 (2019).
33. Papoutsoglou, P. & Moustakas, A. Long non-coding RNAs and TGF- $\beta$  signaling in cancer. *Cancer Sci.* **111**, 2672–2681 (2020).
34. Wang, P. *et al.* Long noncoding RNA lnc-TSI inhibits renal fibrogenesis by negatively regulating the TGF- $\beta$ /SMAD3 pathway. *Sci. Transl. Med.* **10**, eaat2039 (2018).
35. Fan, C.N. *et al.* LncRNA LITATS1 suppresses TGF- $\beta$ -induced EMT and cancer cell plasticity by potentiating T $\beta$ RI degradation. *EMBO J.* **42**, e112806 (2023).
36. Altschul, S.F., Gish, W., Miller, W., Myers, E.W. & Lipman, D.J. Basic local alignment search tool. *J. Mol. Biol.* **215**, 403–410 (1990).
37. Wang, L. *et al.* CPAT: Coding-potential assessment tool using an alignment-free logistic regression model. *Nucleic Acids Res.* **41**, e74 (2013).
38. Dennler, S. *et al.* Direct binding of SMAD3 and SMAD4 to critical TGF beta-inducible elements in the promoter of human plasminogen activator inhibitor-type 1 gene. *EMBO J.* **17**, 3091–3100 (1998).
39. Marvin, D.L. *et al.* Dynamic visualization of TGF- $\beta$ /SMAD3 transcriptional responses in single living cells. *Cancers (Basel)* **14**, 2508 (2022).
40. Padua, D. *et al.* TGF $\beta$  primes breast tumors for lung metastasis seeding through angiopoietin-like 4. *Cell* **133**, 66–77 (2008).
41. Gil, N. & Ulitsky, I. Regulation of gene expression by cis-acting long non-coding RNAs. *Nat. Rev. Genet.* **21**, 102–117 (2020).
42. Sun, Q., Hao, Q. & Prasanth, K.V. Nuclear long noncoding RNAs: Key regulators of gene expression. *Trends Genet.* **34**, 142–157 (2018).
43. Yi, W. *et al.* CRISPR-assisted detection of RNA-protein interactions in living cells. *Nat. Methods* **17**, 685–688 (2020).
44. Zhu, L., Liu, Y., Tang, H. & Wang, P. FOXP3 activated-LINC01232 accelerates the stemness of non-small cell lung carcinoma by activating TGF- $\beta$  signaling pathway and recruiting IGF2BP2 to stabilize TGFBR1. *Exp. Cell Res.* **413**, 113024 (2022).
45. Cheng, D.M. *et al.* Long noncoding RNA-SNHG20 promotes silica-induced pulmonary fibrosis by miR-490-3p/TGFBR1 axis. *Toxicology* **451**, 152683 (2021).
46. Hu, H.Y. *et al.* Long non-coding RNA TCONS\_00814106 regulates porcine granulosa cell proliferation and apoptosis by sponging miR-1343. *Mol. Cell. Endocrinol.* **520**, 111064 (2021).
47. Li, Y.C., Zhao, Z., Sun, D. & Li, Y.F. Novel long noncoding RNA LINC02323 promotes cell growth and migration of ovarian cancer via TGF- $\beta$  receptor 1 by miR-1343-3p. *J. Clin. Lab. Anal.* **35**, e23651 (2021).
48. Zhou, B., Guo, W.D., Sun, C.D., Zhang, B.Y. & Zheng, F. Linc00462 promotes pancreatic cancer invasiveness through the miR-665/TGFBR1-TGFBR2/SMAD2/3 pathway. *Cell Death Dis.* **9**, 706 (2018).
49. Jin, J., Jia, Z.H., Luo, X.H. & Zhai, H.F. Long non-coding RNA HOXA11-AS accelerates the progression of keloid formation via miR-124-3p/TGF $\beta$ R1 axis. *Cell Cycle* **19**, 218–232 (2020).
50. Yang, G. & Lin, C.S. Long noncoding RNA SOX2-OT exacerbates hypoxia-induced cardiomyocytes injury by regulating miR-27a-3p/TGF $\beta$ R1 axis. *Cardiovasc. Ther.* **2020**, 2016259 (2020).
51. Li, Y. *et al.* Long non-coding RNA SBF2-AS1 promotes hepatocellular carcinoma progression through regulation of miR-140-5p-TGFBR1 pathway. *Biochem. Biophys. Res. Commun.* **503**, 2826–2832 (2018).
52. Qi, J., Wu, Y.Y., Zhang, H.J. & Liu, Y.F. LncRNA NORAD regulates scar hypertrophy via miRNA-26a

- mediating the regulation of TGF $\beta$ R1/2. *Adv. Clin. Exp. Med.* **30**, 395–403 (2021).
53. Gilbert, L.A. *et al.* CRISPR-mediated modular RNA-guided regulation of transcription in eukaryotes. *Cell* **154**, 442–451 (2013).
  54. Ransohoff, J.D., Wei, Y.N. & Khavari, P.A. The functions and unique features of long intergenic non-coding RNA. *Nat. Rev. Mol. Cell Biol.* **19**, 143–157 (2018).
  55. Ulitsky, I. & Bartel, D.P. lincRNAs: Genomics, evolution, and mechanisms. *Cell* **154**, 26–46 (2013).
  56. Ogunjimi, A.A. *et al.* Regulation of Smurf2 ubiquitin ligase activity by anchoring the E2 to the HECT domain. *Mol. Cell* **19**, 297–308 (2005).
  57. Kuratomi, G. *et al.* NEDD4-2 (neural precursor cell expressed, developmentally down-regulated 4-2) negatively regulates TGF- $\beta$  (Transforming growth factor- $\beta$ ) signalling by inducing ubiquitin-mediated degradation of SMAD2 and TGF- $\beta$  type I receptor. *Biochem. J.* **386**, 461–470 (2005).
  58. Hedrick, E., Mohankumar, K. & Safe, S. TGF $\beta$ -induced lung cancer cell migration is NR4A1-dependent. *Mol. Cancer Res.* **16**, 1991–2002 (2018).
  59. Hedrick, E. & Safe, S. Transforming growth factor  $\beta$ /NR4A1-inducible breast cancer cell migration and epithelial-to-mesenchymal transition is p38 $\alpha$  (mitogen-activated protein kinase 14) dependent. *Mol. Cell. Biol.* **37**, e00306–e00317 (2017).
  60. Gao, Y. *et al.* LncRNA lncLy6C induced by microbiota metabolite butyrate promotes differentiation of Ly6C<sup>high</sup> to Ly6C<sup>int/neg</sup> macrophages through lncLy6C/C/EBP $\beta$ /Nr4A1 axis. *Cell Discov.* **6**, 87 (2020).
  61. Stroud, J.C., Lopez-Rodriguez, C., Rao, A. & Chen, L. Structure of a TonEBP-DNA complex reveals DNA encircled by a transcription factor. *Nat. Struct. Biol.* **9**, 90–94 (2002).
  62. Lopez, A.M., Pegram, M.D., Slamon, D.J. & Landaw, E.M. A model-based approach for assessing in vivo combination therapy interactions. *Proc. Natl. Acad. Sci. U.S.A.* **96**, 13023–13028 (1999).
  63. Lee, S.D., Woo, S.K. & Kwon, H.M. Dimerization is required for phosphorylation and DNA binding of TonEBP/NFAT5. *Biochem. Biophys. Res. Commun.* **294**, 968–975 (2002).
  64. Guo, K. & Jin, F.G. NFAT5 promotes proliferation and migration of lung adenocarcinoma cells in part through regulating AQP5 expression. *Biochem. Biophys. Res. Commun.* **465**, 644–649 (2015).
  65. Li, J.T. *et al.* Nuclear factor of activated T cells 5 maintained by Hotair suppression of miR-568 upregulates S100 calcium binding protein A4 to promote breast cancer metastasis. *Breast Cancer Res.* **16**, 454 (2014).
  66. Meng, X., Li, Z., Zhou, S., Xiao, S. & Yu, P. miR-194 suppresses high glucose-induced non-small cell lung cancer cell progression by targeting NFAT5. *Thorac. Cancer* **10**, 1051–1059 (2019).
  67. Yang, M.J., Ke, H.G. & Zhou, W. LncRNA RMRP promotes cell proliferation and invasion through miR-613/NFAT5 axis in non-small cell lung cancer. *Oncotargets Ther.* **13**, 8941–8950 (2020).
  68. Lambert, S.A. *et al.* The human transcription factors. *Cell* **172**, 650–665 (2018).
  69. Liu, J. *et al.* TF-PROTACs enable targeted degradation of transcription factors. *J. Am. Chem. Soc.* **143**, 8902–8910 (2021).
  70. Shao, J.W. *et al.* Destruction of DNA-binding proteins by programmable oligonucleotide PROTAC (O<sup>PROTAC</sup>): Effective targeting of LEF1 and ERG. *Adv. Sci. (Weinh)* **8**, 2102555 (2021).
  71. Maruyama, R. & Yokota, T. Knocking down long noncoding RNAs using antisense oligonucleotide gapmers. *Methods Mol. Biol.* **2176**, 49–56 (2020).
  72. Dey, S.K. & Jaffrey, S.R. RIBOTACs: Small molecules target RNA for degradation. *Cell Chem. Biol.* **26**, 1047–1049 (2019).
  73. Fan, C. *et al.* OVOL1 inhibits breast cancer cell invasion by enhancing the degradation of TGF- $\beta$  type I receptor. *Signal Transduct. Target. Ther.* **7**, 126 (2022).
  74. Wang, Q. *et al.* Broadening the reach and investigating the potential of prime editors through fully viral gene-deleted adenoviral vector delivery. *Nucleic Acids Res.* **49**, 11986–12001 (2021).
  75. Sinha, A. *et al.* Visualizing dynamic changes during TGF- $\beta$ -induced epithelial to mesenchymal transition. *Methods Mol. Biol.* **2488**, 47–65 (2022).
  76. Rappsilber, J., Mann, M. & Ishihama, Y. Protocol for micro-purification, enrichment, pre-fractionation and storage of peptides for proteomics using StageTips. *Nat. Protoc.* **2**, 1896–1906 (2007).
  77. Daniel Salas-Lloret, C.v.d.M., Easa Nagamalleswari, Ekaterina Gracheva, Arnoud H. de Ru, H. Anne Marie Otte, Peter A. van Veelen, Andrea Pichler, Joachim Goedhart, Alfred C.O. Vertegaal, Román González-Prieto SUMO activated target traps (SATTs) enable the identification of a comprehensive E3-specific SUMO proteome. *bioRxiv* 2022.2006.2022.497173, (2022).
  78. Tyanova, S., Temu, T. & Cox, J. The MaxQuant computational platform for mass spectrometry-based shotgun proteomics. *Nat. Protoc.* **11**, 2301–2319 (2016).
  79. Tyanova, S. *et al.* The Perseus computational platform for comprehensive analysis of (prote)omics data. *Nat. Methods* **13**, 731–740 (2016).
  80. Subramanian, A. *et al.* Gene set enrichment analysis: A knowledge-based approach for interpreting genome-wide expression profiles. *Proc. Natl. Acad. Sci. U.S.A.* **102**, 15545–15550 (2005).

81. Ren, J., Liu, S., Cui, C. & Ten Dijke, P. Invasive behavior of human breast cancer cells in embryonic zebrafish. *J. Vis. Exp.* **122**, 55459 (2017).
82. Perez-Riverol, Y. *et al.* The PRIDE database and related tools and resources in 2019: Improving support for quantification data. *Nucleic Acids Res.* **47**, D442–D450 (2019).

## Supplementary information

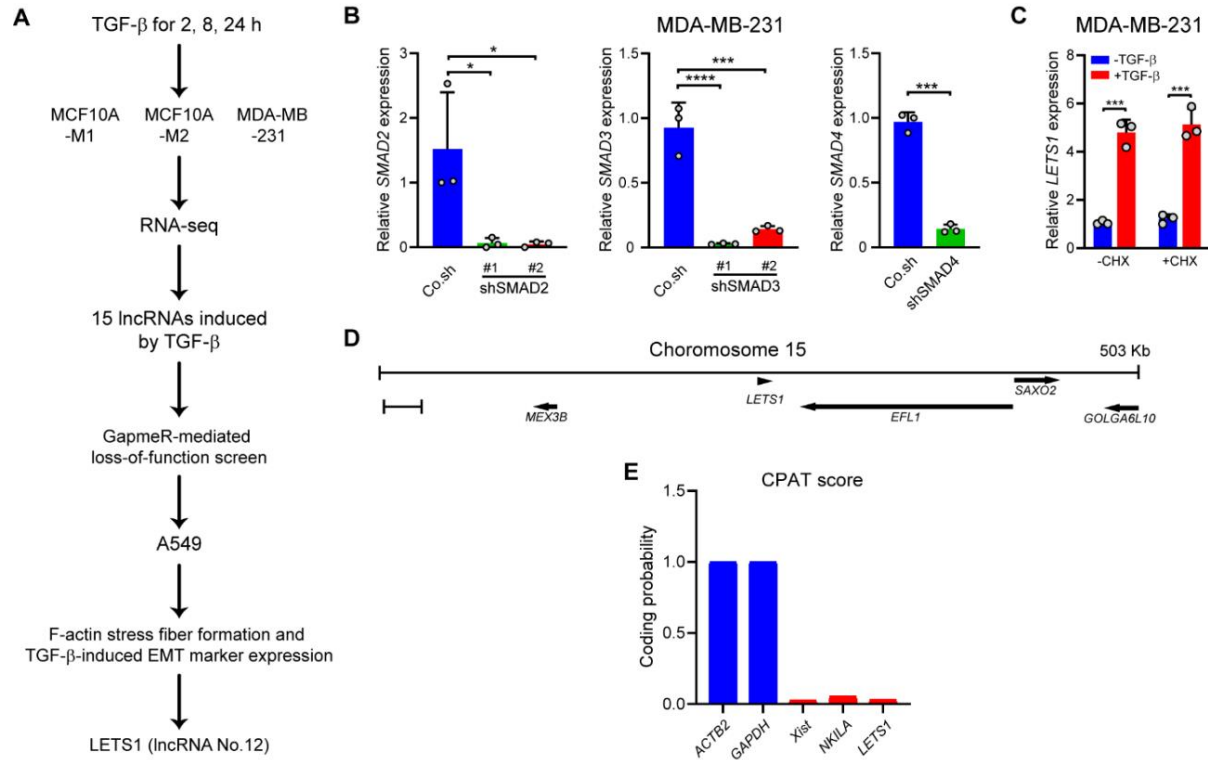


**Fig. S1. *LETS1* is a TGF- $\beta$ -induced lncRNA.** (A) Workflow showing the screening strategy to identify TGF- $\beta$ -induced *LETS1* that functions as an activator of EMT. (B) Expression of *SMAD2*, *SMAD3* or *SMAD4* in MDA-MB-231 cells upon shRNA-mediated *SMAD2*, *SMAD3*, or *SMAD4* knockdown. RT-qPCR results are shown as means  $\pm$  SD from three biological replicates in one independent experiment and representative of at least three independent experiments. (C) Quantification of *LETS1* expression in MDA-MB-231 cells pre-treated with cycloheximide and stimulated with TGF- $\beta$  or vehicle. RT-qPCR results are shown as means  $\pm$  SD from three biological replicates in one independent experiment and representative of two independent experiments. (D) Schematic representation of the genomic location of *LETS1* and its neighboring genes. The arrows indicate the direction of transcription. (E) The predicted coding potential of protein-coding mRNAs (*ACTB2* and *GAPDH*), well-annotated lncRNAs (*Xist* and *NKILA*) and *LETS1*. In (B, left and middle), significance was assessed using one-way ANOVA followed by Dunnett's multiple comparisons test. In (B, right) and (C), significance was assessed using unpaired Student's t test. \*,  $0.01 < p < 0.05$ ; \*\*\*,  $0.0001 < p < 0.001$ ; \*\*\*\*,  $p < 0.0001$ .

The lncRNA *LETS1* promotes TGF- $\beta$ -induced EMT and cancer cell migration by transcriptionally activating a T $\beta$ RI-stabilizing mechanism

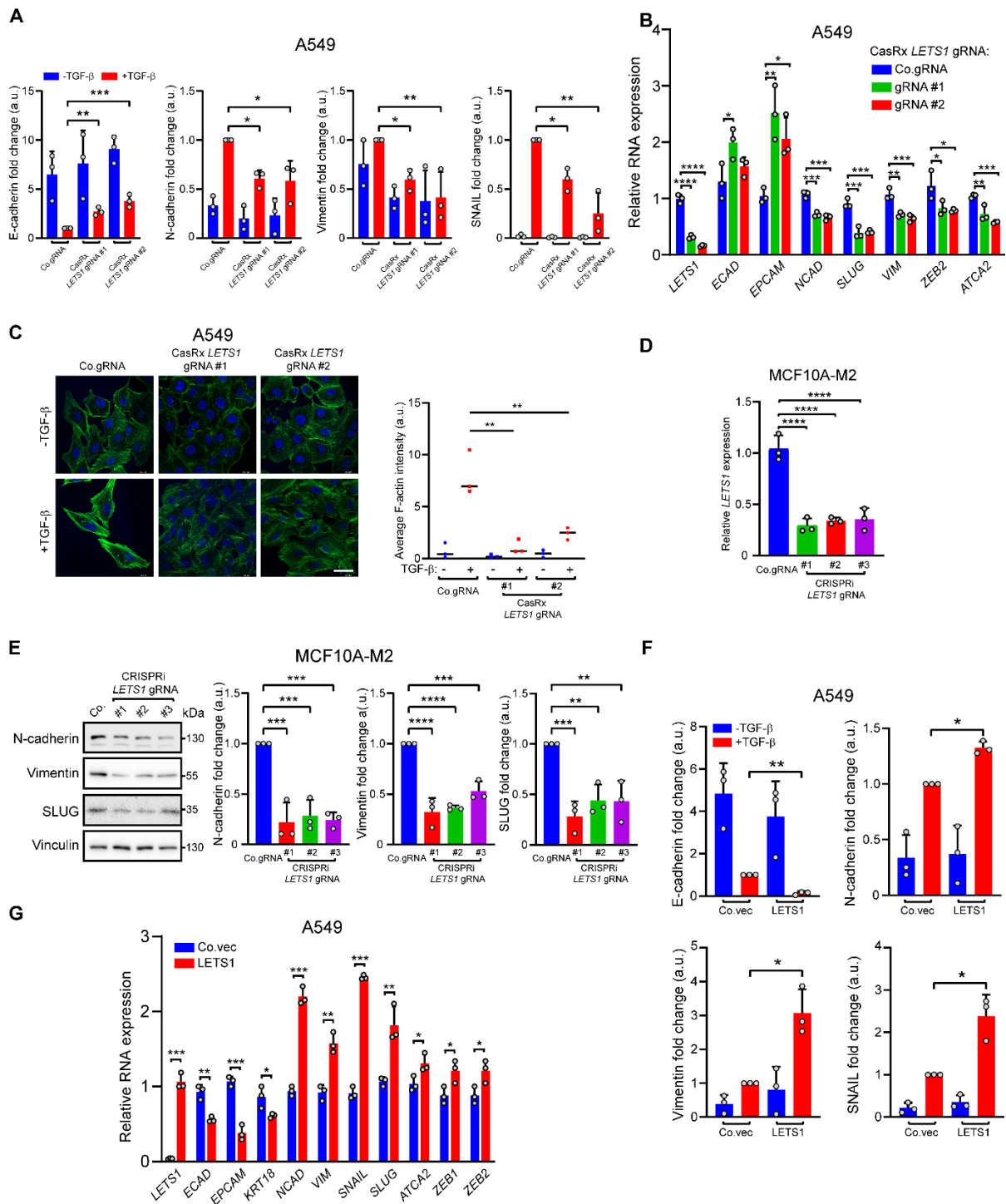


**Fig. S2. *LETS1* promotes TGF- $\beta$ -induced EMT.** (A) Quantification results of western blotting in Fig. 2A. Statistical results are means  $\pm$  SD from three independent experiments. a.u., arbitrary units. (B) Expression of EMT markers in A549 cells upon CRISPR/CasRx-mediated *LETS1* knockdown. RT-qPCR results are shown as means  $\pm$  SD from three biological replicates in one independent experiment and representative of at least three independent experiments. (C) Fluorescent staining for F-actin in A549 cells upon *LETS1* depletion by CRISPR/CasRx. Co.gRNA, empty vector. DAPI staining was performed to visualize nuclei. Scale bar, 38.8  $\mu$ m. Quantification of average F-actin intensity is shown as means  $\pm$  SD from three independent experiments. (D) *LETS1* expression in MCF10A-M2 cells upon CRISPRi-mediated *LETS1* knockdown. RT-qPCR results are shown as means  $\pm$  SD from three biological replicates in one independent experiment and representative of at least three independent experiments. (E) Immunoblotting for N-cadherin, Vimentin, and SLUG in MCF10A-M2 cells expressing the CRISPRi construct and empty vector (Co.) or *LETS1*-targeting guide RNA (gRNA). Vinculin, loading control. Quantification results are shown as means  $\pm$  SD from three independent experiments. (F) Quantification results of western blotting in Fig. 2B. Statistical results are means  $\pm$  SD from three independent experiments. (G) Expression of EMT markers in A549 cells upon *LETS1* ectopic expression. RT-qPCR results are shown as means  $\pm$  SD from three biological replicates in one



independent experiment and representative of at least three independent experiments. In (A), (E) and (F), significance was assessed using paired Student's *t* test. In (B), (C) and (D), significance was assessed using one-way ANOVA followed by Dunnett's multiple comparisons test. In (G), significance was assessed using unpaired Student's *t* test. \*,  $0.01 < p < 0.05$ ; \*\*,  $0.001 < p < 0.01$ ; \*\*\*,  $0.0001 < p < 0.001$ ; \*\*\*\*,  $p < 0.0001$ .

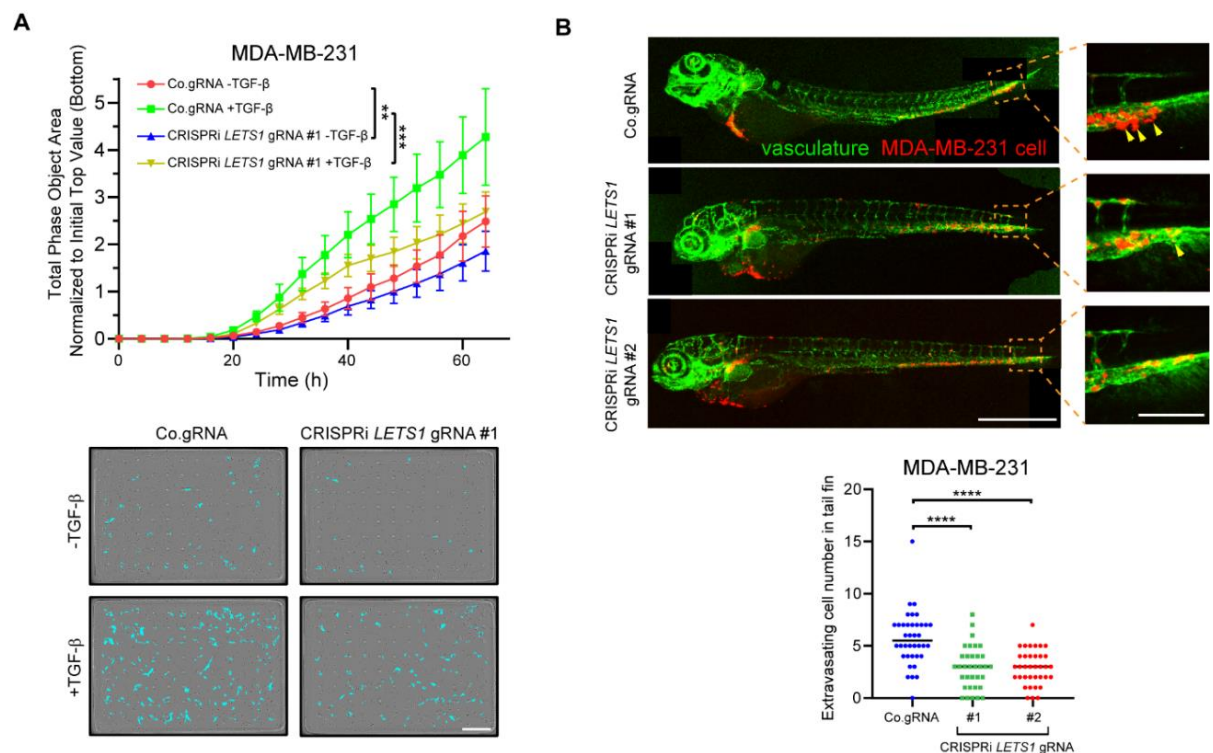


**Fig. S3. *LETS1* knockdown attenuates TGF- $\beta$ -induced cell migration and extravasation.** (A) An IncuCyte chemotactic migration assay was performed with MDA-MB-231 cells upon CRISPRi-mediated *LETS1* depletion. Cells that migrated to the bottom of chambers are marked in blue in the images. The migration results are expressed as means  $\pm$  SD from six biological replicates in one independent experiment and representative of at least three independent experiments. Scale bar, 400  $\mu$ m. Significance was assessed using two-way ANOVA followed by Tukey's multiple comparisons test. \*\*,  $0.001 < p < 0.01$ ; \*\*\*,  $0.0001 < p < 0.001$ . (B) In vivo zebrafish extravasation experiments with MDA-MB-231 cells upon CRISPRi-mediated *LETS1* depletion. Extravasated breast cancer cells in the zoomed tail fin area are indicated with yellow arrows. Numbers of extravasated cell are expressed as means  $\pm$  SD. Scale bars, 309.1  $\mu$ m (whole fish); 154.5  $\mu$ m (enlargements). N = at least 30 fish per treatment group. Images are representative of two independent experiments. Significance was assessed using one-way ANOVA followed by Dunnett's multiple comparisons test. \*\*\*\*,  $p < 0.0001$ . *LETS1* knockdown efficiency is shown in fig. S5A.

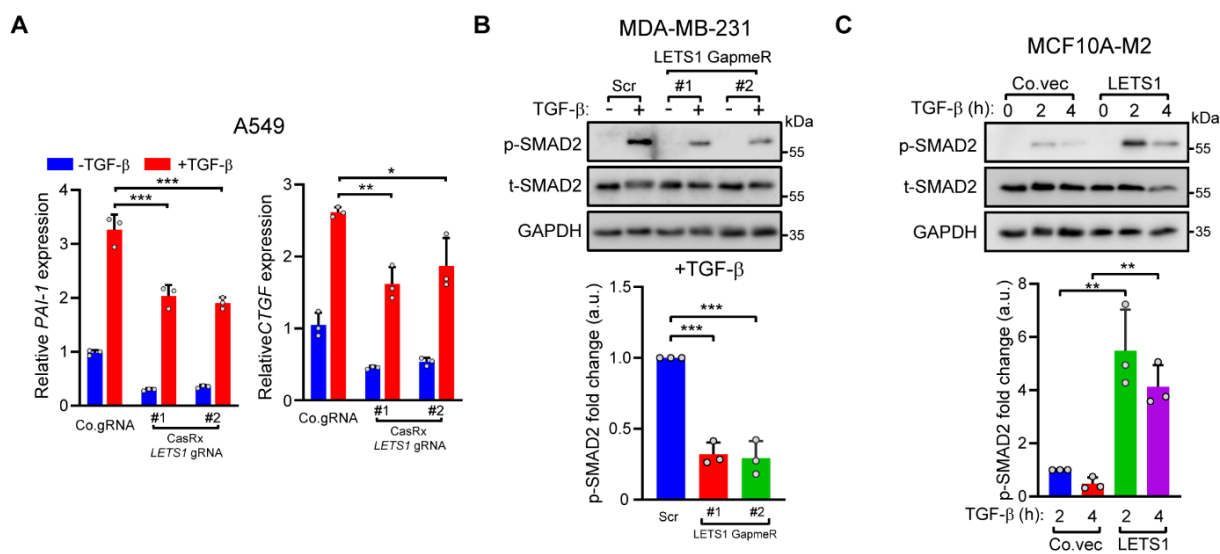


**Fig. S4. *LETS1* knockdown attenuates TGF- $\beta$ /SMAD signaling.** (A) *PAI-1* and *CTGF* expression in A549 cells upon

The lncRNA *LETS1* promotes TGF- $\beta$ -induced EMT and cancer cell migration by transcriptionally activating a T $\beta$ RI-stabilizing mechanism

CRISPR/CasRx-mediated *LETS1* depletion. RT-qPCR results are shown as means  $\pm$  SD from three biological replicates in one independent experiment and representative of at least three independent experiments. (B, C) Immunoblotting for phosphorylated (p-) and total (t-) SMAD2 in TGF- $\beta$ -stimulated MDA-MB-231 or MCF10AM2 cells in which *LETS1* was knocked down by GapmeR (MDA-MB-231) or in which *LETS1* was overexpressed (MCF10A-M2) Blots are representative of at least three independent experiments and statistical results are means  $\pm$  SD from three independent experiments. In (A), significance was assessed using one-way ANOVA followed by Dunnett's multiple comparisons test. In (B) and (C), significance was assessed using paired Student's *t* test. \*, 0.01 < *p* < 0.05; \*\*, 0.001 < *p* < 0.01; \*\*\*, 0.0001 < *p* < 0.001.

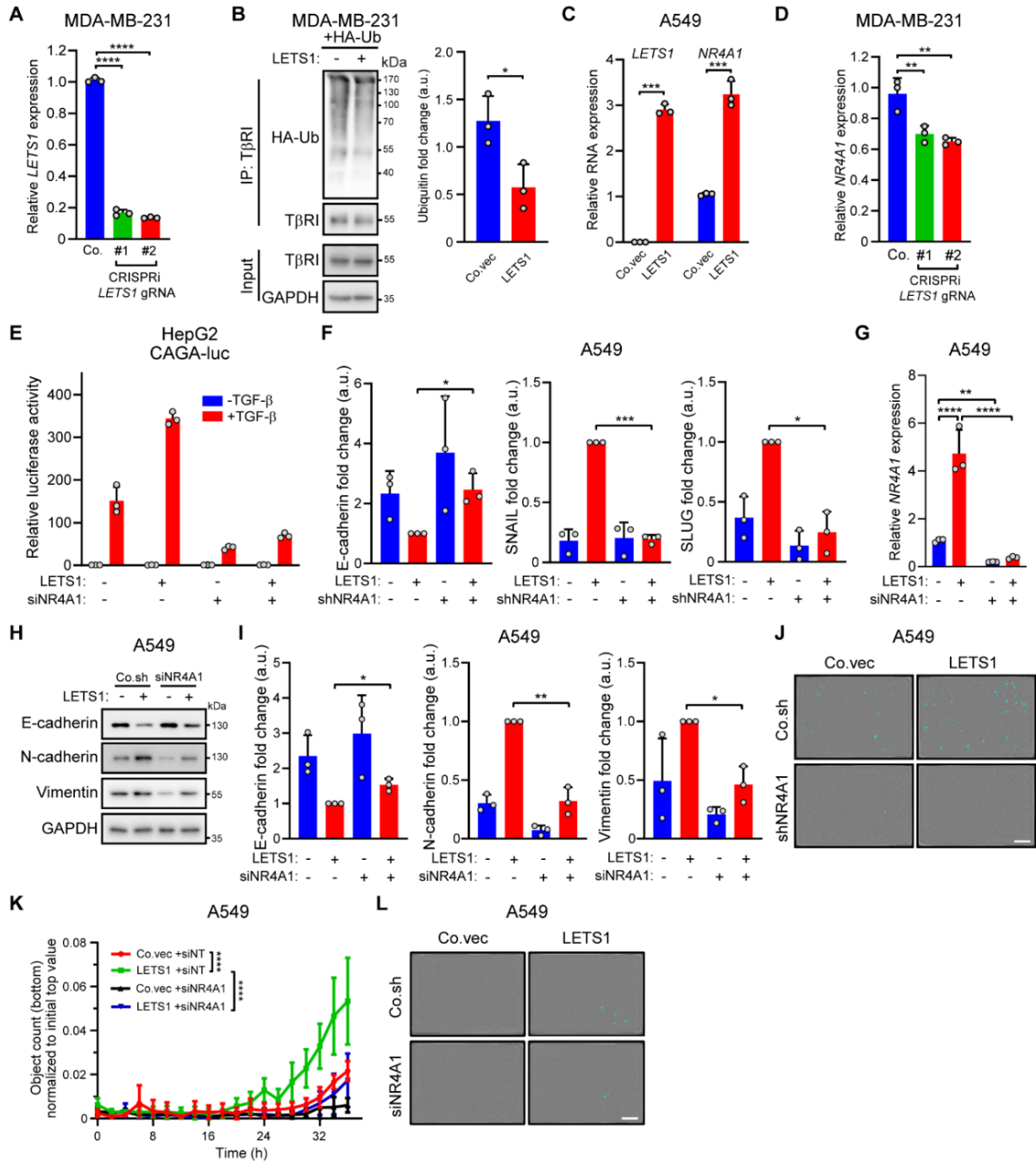


**Fig. S5. *NR4A1* is induced by *LETS1*.** (A) *LETS1* expression in MDA-MB-231 cells upon CRISPRi-mediated *LETS1* knockdown. RT-qPCR results are shown as means  $\pm$  SD from three biological replicates in one independent experiment and representative of at least three independent experiments. (B) Immunoblotting for HA and T $\beta$ RI in total lysates (input) and T $\beta$ RI immunoprecipitates (IP) from MDA-MB-231 cells expressing HA-ubiquitin (HA-Ub) and empty vector (Co.vec) or *LETS1*. Ubiquitin was quantified in the T $\beta$ RI immunoprecipitates. Quantitative data are means  $\pm$  SD from three independent experiments. (C) *LETS1* and *NR4A1* expression in A549 cells upon ectopic *LETS1* expression. RT-qPCR results are shown as means  $\pm$  SD from three biological replicates in one independent experiment and representative of at least three independent experiments. (D) *NR4A1* expression in MDA-MB-231 cells upon CRISPRi-mediated *LETS1* knockdown. RT-qPCR results are shown as means  $\pm$  SD from three biological replicates in one independent experiment and representative of at least three

independent experiments. (E) Luciferase activity in TGF- $\beta$ -stimulated HepG2 cells transfected with the expression construct for the SMAD3/4 transcriptional reporter CAGA-luc plus the LETS1 ectopic expression construct and the NR4A1-targeting siRNA as indicated. The relative luciferase activities are representative of at least three independent experiments and expressed as means  $\pm$  SD from three wells with cells per treatment group in one experiment. (F) Quantification results of western blotting in Fig. 4G. Statistical results are means  $\pm$  SD from three independent experiments. (G) *NR4A1* expression in MDA-MB-231 cells with LETS1 ectopic expression and siRNA-mediated NR4A1 knockdown. RT-qPCR results are shown as means  $\pm$  SD from three biological replicates in one independent experiment and representative of two independent experiments. (H) Immunoblotting for E-cadherin, N-cadherin, and Vimentin in A549 cells in which LETS1 was overexpressed and NR4A1 was knocked down by siRNA as indicated. Blots are representative of three independent experiments. (I) Quantification results of western blotting in fig. S5H. Statistical results are means  $\pm$  SD from three independent experiments. (J) The representative images of migrated cells in Fig. 4H. The cells that migrated to the bottom of chambers are marked in blue in the images. Scale bar, 400  $\mu$ m. (K) Quantification of migrated cells in IncuCyte chemotactic migration assays using A549 cells with LETS1 overexpression and NR4A1 knockdown by siRNA as indicated. The migration results are expressed as means  $\pm$  SD from five biological replicates in one independent experiment and representative of two independent experiments. (L) The representative images of migrated cells in fig. S5K. The cells that migrated to the bottom of chambers are marked in blue in the images. Scale bar, 400  $\mu$ m. In (A), (D), and (G), significance was assessed using one-way ANOVA followed by Dunnett's multiple comparisons test. In (C), significance was assessed using unpaired Student's *t* test. In (B), (F) and (I), significance was assessed using paired Student's *t* test. In (K), significance was assessed using two-way ANOVA followed by Tukey's multiple comparisons test. \*, 0.01 < *p* < 0.05; \*\*, 0.001 < *p* < 0.01; \*\*\*, 0.0001 < *p* < 0.001; \*\*\*\*, *p* < 0.0001.

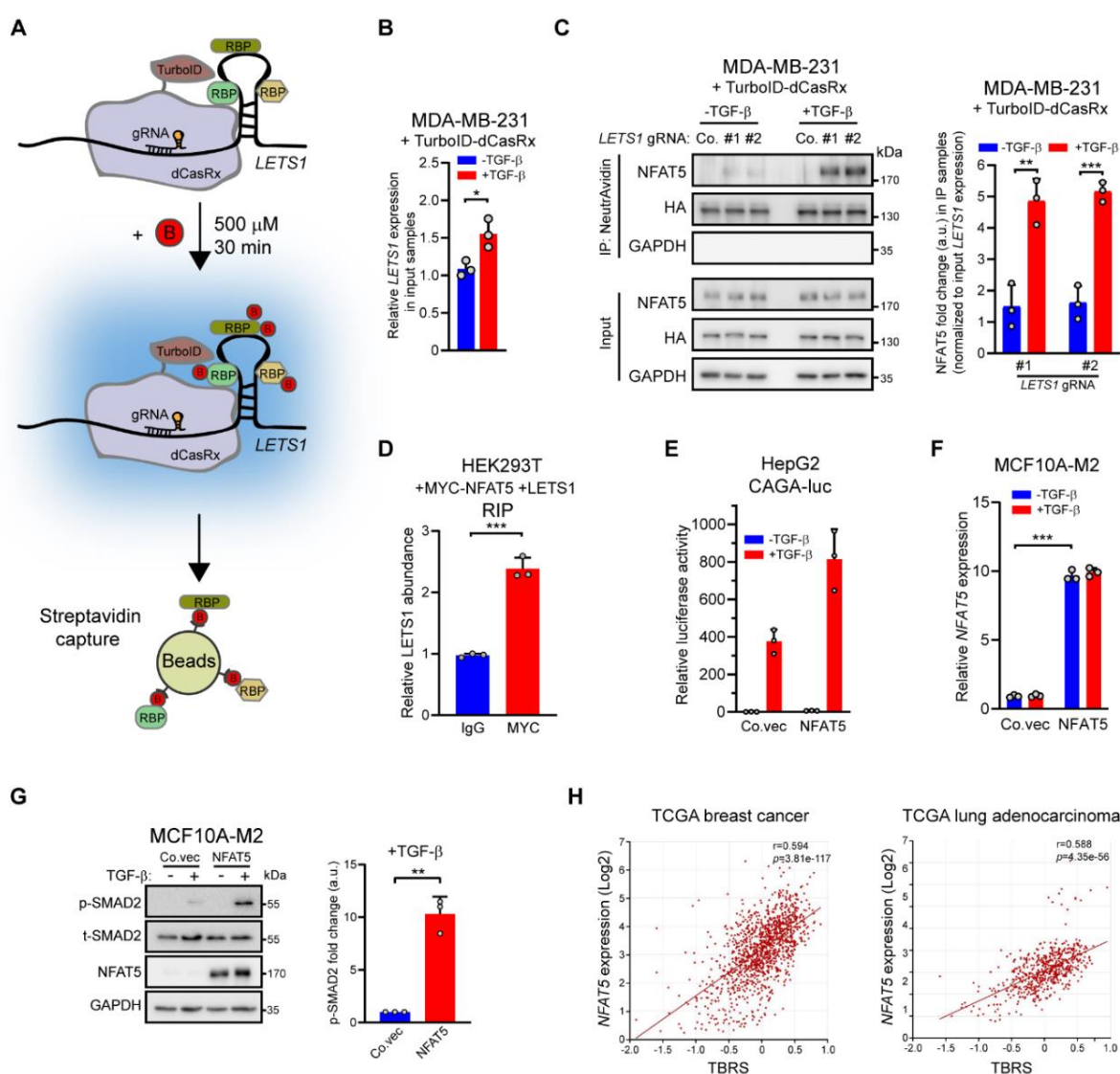


**Fig. S6. NFAT5 potentiates TGF- $\beta$ –SMAD signaling.** (A) Scheme of the CARPID workflow. B: biotin; RBP: RNA binding protein. (B) *LETS1* expression in MDA-MB-231 cells with TurboID–dCasRx expression and stimulated with TGF- $\beta$  or vehicle. RT-qPCR results are shown as means  $\pm$  SD from three biological replicates in one independent experiment and representative of two independent experiments. (C) Interactions between LETS1 and NFAT5 were analyzed by CARPID in MDA-MB-231 with TurboID–dCasRx expression. Western blotting was performed to detect NFAT5 expression in whole-cell lysates (Input)

The lncRNA *LETS1* promotes TGF- $\beta$ -induced EMT and cancer cell migration by transcriptionally activating a T $\beta$ RI-stabilizing mechanism

and immunoprecipitates (IP). Blots are representative of at least three independent experiments. NFAT5 abundance in IP samples was normalized to *LETS1* expression in input samples. Statistical results are means  $\pm$  SD from three independent experiments. (D) RIP assay quantifying *LETS1* abundance in MYC immunoprecipitates from HEK293T cells with MYCN4A1 and *LETS1* ectopic expression. *LETS1* abundance in MYC immunoprecipitates is presented as relative to that in IgG immunoprecipitates. RT-qPCR results are shown as means  $\pm$  SD from three biological replicates in one independent experiment and representative of two independent experiments (E) Luciferase activity in TGF- $\beta$ -stimulated HepG2 cells transfected with the expression construct for the SMAD3/4 transcriptional reporter CAGA-luc plus the NFAT5 ectopic expression construct. The relative luciferase activities are representative of at least three independent experiments and expressed as means  $\pm$  SD from three wells with cells per treatment group in one experiment. (F) *NFAT5* expression in MCF10A-M2 cells with NFAT5 ectopic expression. The RT-qPCR results are shown as means  $\pm$  SD from three biological replicates in one independent experiment and representative of at least three independent experiments. (G) Immunoblotting for phosphorylated (p-) and total (t-) SMAD2 and NFAT5 in TGF- $\beta$ -stimulated MCF10A-M2 cells with NFAT5 overexpression. Quantitative data show the abundance of p-SMAD2 relative to t-SMAD2. Results are means  $\pm$  SD from three independent experiments. (H) Correlations between NFAT5 and the TGF- $\beta$  gene response signature (TBRS) in patients with breast cancer or lung adenocarcinoma. In (B), (D), and (F), significance was assessed using unpaired Student's *t* test. In (C) and (G), significance was assessed using paired Student's *t* test. In (H), statistical analysis was performed using Pearson's correlation test. \*, 0.01 < *p* < 0.05; \*\*, 0.001 < *p* < 0.01; \*\*\*, 0.0001 < *p* < 0.001.

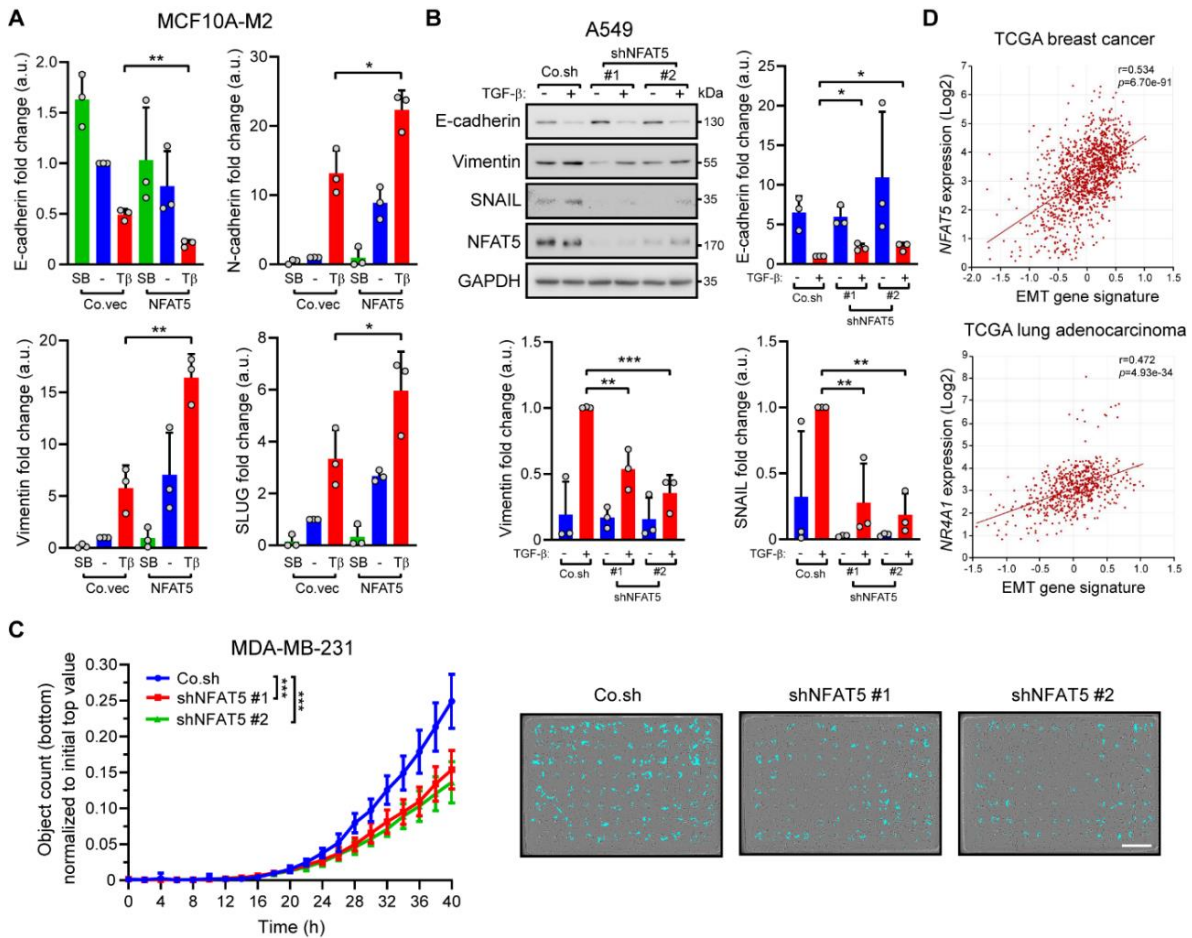


**Fig. S7. NFAT5 potentiates TGF- $\beta$ -induced EMT and cell migration.** (A) Quantification results of western blotting in Fig. 5H. Statistical results are means  $\pm$  SD from three independent experiments. (B) Immunoblotting for E-cadherin, Vimentin, SNAIL, and NFAT5 in A549 cells upon NFAT5 knockdown and treated with vehicle or TGF- $\beta$  (T $\beta$ ). Co.sh, empty vector. Blots are representative of at least three independent experiments. Quantification results are means  $\pm$  SD from three independent experiments. (C) Quantification of migrated cells in IncuCyte chemotactic migration assays using MDA-MB231 cells upon NFAT5 knockdown. The cells that migrated to the bottom of chambers are marked in blue in the images. The migration results are expressed as means  $\pm$  SD from 12 biological replicates in one independent experiment and representative of two independent experiments. Scale bar, 400  $\mu$ m. (D) Correlations between *NFAT5* and the EMT signature in patients with breast cancer or lung adenocarcinoma. In (A) and (B), significance was assessed using paired Student's *t* test. In (C), significance was assessed using two-way ANOVA followed by Tukey's multiple comparisons test. In (D), statistical analysis was performed using Pearson's correlation test. \*, 0.01 < *p* < 0.05; \*\*, 0.001 < *p* < 0.01; \*\*\*, 0.0001 < *p* < 0.001.

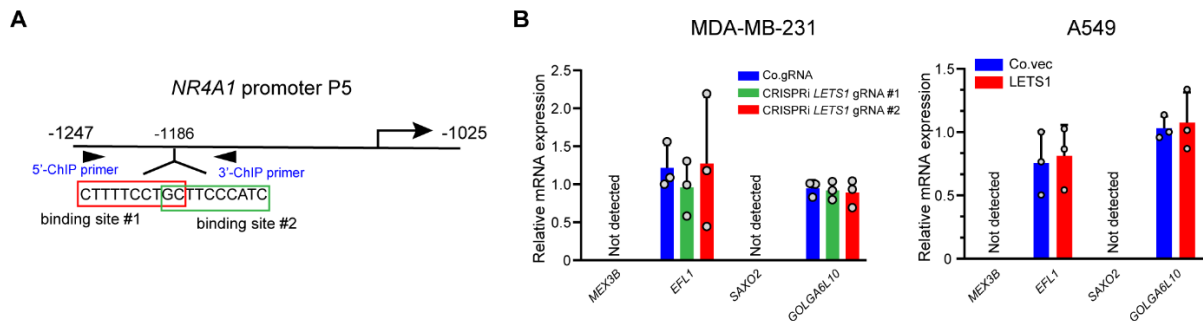


**Fig. S8. The expression of *LETS1* nearby genes is not affected upon *LETS1* misexpression.** (A) Schematic representation of *NR4A1* promoter P5. The two putative binding sites of NFAT5 and the binding sites of ChIP primers are shown. (B) Quantification of *LETS1* neighboring gene expression in A549 cells with *LETS1* ectopic expression and MDA-MB-231 cells upon CRISPRi-mediated *LETS1* knockdown. RT-qPCR results are shown as means  $\pm$  SD from three biological replicates in one independent experiment and representative of two independent experiments.

Supplementary tables are online at <https://www.science.org/doi/10.1126/scisignal.adf1947>.